



Title	Study of amino-acid crystal fermentation : Biochemical analysis of stress responses of Escherichia coli in a model culture system and an improvement of the fermentation process
Author(s)	奥谷, 聡志
Citation	大阪大学, 2015, 博士論文
Version Type	VoR
URL	https://doi.org/10.18910/52276
rights	
Note	

The University of Osaka Institutional Knowledge Archive : OUKA

<https://ir.library.osaka-u.ac.jp/>

The University of Osaka

Study of amino-acid crystal fermentation:

**Biochemical analysis of stress responses of *Escherichia coli* in a model culture system
and an improvement of the fermentation process**

アミノ酸晶析発酵に関する研究：

モデル培養系における大腸菌のストレス応答の生化学的解析と発酵プロセスの改良

A doctoral thesis

Satoshi Okutani

Research Institute for Bioscience Products & Fine Chemicals
Ajinomoto Co., Inc.

Department of Biological Sciences, Graduate School of Science
Laboratory of Regulation of Biological Reactions, Institute for Protein Research
Osaka University

February, 2015

Contents

Abbreviation.....	1
General Introduction	2
Bacterial response to stress.....	3
Industrial amino acid production.....	5
Fermentation process and amino-acid crystal fermentation	8
Modification of culture agitation for crystal fermentation	14
Study 1. Mechanical stress and damage to <i>E. coli</i> cells by PVC particles.....	16
Introduction	17
Materials and methods	18
Discussion	33
Study 2. Fe-S cluster assembly machinery responsible for relief of the mechanical stress.....	36
Introduction	37
Materials and methods	41
Results	47
Discussion	61
Study 3. Development of a culture process for efficient amino acid crystal fermentation.....	64
Introduction	65
Materials and Methods.....	66
Results	68
Discussion	75
Summary (和文)	76
References	79

Abbreviation

ATP;	adenosine triphosphate
BCECF-AM;	2',7'-bis-(2-carboxyethyl)-5-(and-6)-carboxyfluorescein, acetoxymethyl ester
CT;	culture time
Fe-S;	iron-sulfur
HPLC;	high performance liquid chromatography
IPTG;	isopropyl β -D-1-thiogalactopyranoside
ISC;	iron-sulfur cluster
LB;	Luria broth
MC;	methyl cellulose
MOPS;	3-Morpholinopropanesulfonic acid
MTT;	3-(4,5-dimethylthiazolyl-2)-2,5-diphenyltetrazolium bromide
NADPH;	nicotinamide-adenine dinucleotide phosphate, reduced form
OD;	optical density
ODS column;	octa decyl silyl column
PMS;	phenazine methosulfate
PVC;	polyvinyl chloride
ROS;	reactive oxygen species
SDS-PAGE;	sodium dodecyl sulfate poly-acrylamide gel electrophoresis
SUF;	sulfur mobilization
TEM;	transmission electron microscopy

General Introduction

Bacterial response to stress

Bacteria live under various environmental conditions and encounter many different stresses during their growth and survival. These stresses can be divided into environmental (temperature, acid, or osmotic pressure), physicochemical, or starving stresses. The bacteria sense these and exhibit various characteristics that enable them to endure these stresses.

It was initially hypothesized that bacterial cells respond to environmental stress conditions by maintaining the level of membrane fluidity by changing the lipid composition of the inner or outer membrane. Bacteria accumulate low molecular unsaturated lipids in the inner membrane under temperatures lower or higher than optimal growth conditions and accumulate high molecular saturated lipids under optimal growth conditions. In recent years, moreover, the stress adaptation of the bacterial cell was thought to control the expression of genes involved in bacterial defense mechanisms through the production of shock proteins or stress proteins. *E. coli* responds to stress conditions by activating small or large groups of genes that are under the control of common regulator proteins. Stress conditions result in the accumulation of these regulator proteins and the subsequent transcription of many genes allows cells to cope with specific stress situations, conferring stress tolerance and survival (Abee, T. and Wouters, J. A., 1999, Chung, H. J., et al 2006).

Bacteria respond to heat stress by inducing the production of heat shock proteins. These proteins function as molecular chaperons that stabilize non-native polypeptides that are generated by translation during protein synthesis or denaturation of existing proteins by heat stress. In addition, some of these heat shock proteins are proteases, which function in the digestion and removal of irreversible heat-damaged

polypeptides and assist in cell growth and motility under normal and stress conditions (Morris, J. G., 1993). Furthermore, some heat shock proteins are necessary for growth under high temperature conditions and play a role in numerous cellular processes such as proteolysis, cell wall synthesis, and plasmid DNA replication (Yura, T., et al 1993, Georgopoulos, C., and Welch, W. J., 1993). DnaK, DnaJ, GrpE, GroEL, and GroES have been identified as heat-inducible molecular chaperons in *E. coli* (Chung, H. J., et al 2006). The primary function of these chaperones is to regulate protein folding and control unfolded/misfolded proteins to ensure re-folding and proper assembly. The heat shock proteins are induced under certain stress conditions, e.g., heat, acid, and oxidative stress.

Oxidative stress caused by reactive oxygen species (ROS) is coordinated by several regulators in *E. coli*. Superoxide dismutase and catalase genes, regulated by OxyR and SoxRS, are two major oxidative stress regulators. OxyR and SoxR undergo conformational changes due to stress and consequently control the expression level of cognate genes. OxyR regulates approximately 30 genes and most of them code for metabolic enzymes or antioxidant enzymes that play a role in the reorganization of cellular metabolism under stress conditions. SoxR is converted by the one-electron oxidation of iron-sulfur (Fe-S) clusters. Oxidized SoxR then activates protein translation of SoxS, which subsequently induces transcription of the structural genes of SoxRS (Abee, T. and Wouters, J. A., 1999, Chung, H. J., et al 2006).

As noted above, when bacteria are exposed to several environmental stresses, various reactions are observed in response to stress level. The bacterial stress response is complex, versatile, and robust. Bacteria have a wide variety of mechanisms that enable, growth and survival under a broad range of environmental conditions. In this

thesis, we studied bacterial response to mechanical stress by particles of amino acid crystals formed during fermentation.

Industrial amino acid production

Amino acids are the building blocks of proteins and are essential for all metabolic processes; thus they are fundamental for life. Amino acids play a major role in flavor, nutrition, physiology, and reactivity. L-glutamate is the most widely produced and consumed amino acid, which is converted into mono-sodium glutamate and used as a flavor enhancer. The annual mono-sodium glutamate market is 2,500,000 tons (Becker, J., and Wittmann, C., 2012). L-lysine, DL-methionine, L-threonine, and L-tryptophan are mainly used in animal nutrition because these essential amino acids tend to be deficient in natural feedstuffs. The annual L-lysine, L-threonine, and L-tryptophan markets are 1,950,000 tons, 330,000 tons, and 9,000 tons, respectively (Ajinomoto Co., Inc. estimate 2012).

Table 1-1 shows the production methods of each amino acid. There are four general methods to produce amino acids for commercial use (Addison, A., 2004, Sano, C., 2009):

1) Extraction

Natural sources containing a high concentration of amino acids are used in the extraction procedure. Crude amino acid is obtained from their natural sources by hydrolysis with strong acid and purified using a strongly acidic ion exchange resin. Industrial manufacturing of amino acids by extraction began with L-glutamate production from wheat gluten when Ajinomoto launched its sodium salt in 1909. This method has since been replaced by fermentation. Today, the extraction process

is used for tyrosine and cysteine production, which have suitable natural sources, providing the most economical process.

2) Chemical synthesis

Amino acids are produced from their precursors using chemical synthesis, which yields a racemic mixture of amino acid enantiomers. Glycine and DL-methionine are commonly produced using this method.

3) Fermentation

Fermentation of amino acids makes use of specific mutants of a microorganism. A carbon (sugar) and nitrogen source (ammonia) are used in this biological process to produce amino acids. Currently, the fermentation method is widely applied because only L-form amino acids are produced. Compared with the three other methods mentioned here, this method is the most suitable for scaling up to industrial-level production.

4) Enzymatic catalysis

In this procedure, a precursor is converted to the target amino acid using a few enzymes, thus eliminating the long process emanating from the use of raw materials, such as sugar fermentation. This method offers the advantage that the precursor can be supplied stably and at low cost.

Table 1-1 Industrial manufacturing method for each amino acid

Black circles (●) indicate crystal fermentation used currently or in the near future

Amino acid	Industrial Manufacturing method			
	1) extraction	2) chemical	3) fermentation	4) enzymatic
L-Glu			●	
L-Lys			○	
L-Thr			●	
L-Phe		○	●	○
L-Gln			●	
L-Arg			○	
L-Trp			●	○
L-Val		○	●	
L-His			●	
L-Ile			●	
L-Pro			○	
L-Ser			○	○
L-Asp				○
L-Cys	○		●	○
L-Ala		○		○
L-Asn	○			
DL-Met		○		
Gly		○		
L-Leu	○		●	
L-Tyr	○		●	

(Addison, A., 2004, 日本必須アミノ酸協会資料 2000, revision)

Fermentation process and amino-acid crystal fermentation

The target amino acid is produced using specially selected microorganisms that will selectively produce only that amino acid in the biological fermentation process. Through cultivation, the sugar sources are converted into amino acid by a continuous multistep enzymatic reaction inside the bacterial producer (Fig. 1-1).

In 1956, the first industrial fermentation technology was constructed on L-glutamate fermentation by *Corynebacterium glutamicum* (Kinoshita, S., et al 1957, Sano, C., 2009). L-glutamine produced by fermentation process using *C. glutamicum* was launched as sodium salt in the late 1950s. Subsequently, *Escherichia coli* has also been used successfully for most L-amino acid production, such as L-lysine, L-threonine, L-tryptophan, L-glutamine, L-phenylalanine, and so on (Thomas, H., 2003; Wolfgang, L., et al 2005; Mitsuhashi, S., 2014).

The construction of microorganisms yielding high performance amino acid production is one of the fundamental technologies for optimization of the biotechnological fermentation process. In the early stages, an iterative method of random mutagenesis and selection was the only way to obtain high performance cell line. However, accumulation of detrimental mutations of strains caused growth retardation, enhanced nutrient demand, weakened stress tolerance, and other degradations. This random mutation method limits industrial production.

New practical approaches use a range of DNA recombinant technology to improve on the classical methods of stain breeding. Comprehensive control of interacting metabolic flux in complex bacterial cells is required in amino acid fermentation. Recently, considerable improvement in amino acid production was achieved by systematic metabolism engineering, which profiles intracellular metabolic

and model-based designs based on strong omics technology. Metabolic engineering has thus become an indispensable technology to improve practical industrial strains (Iwatani, S., 2008).

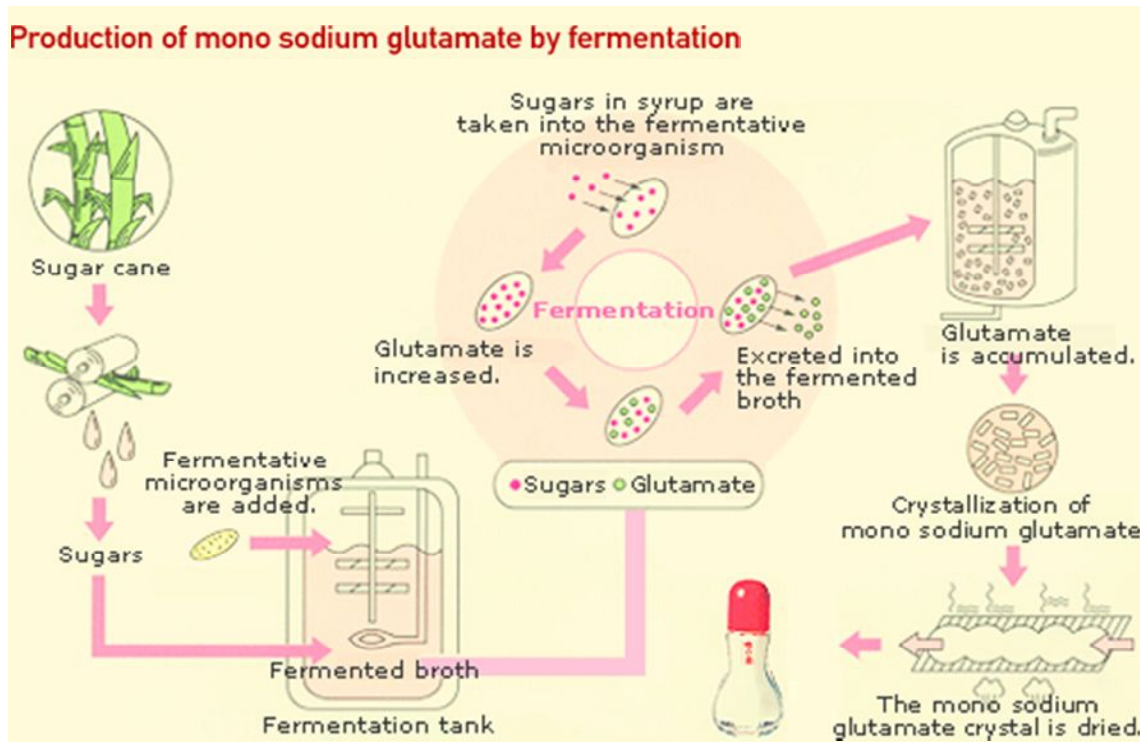
Fig. 1-2 shows a schematic of a fermentation tank. Bacterial cells are stirred by an agitation blade to maintain medium homogeneity and increase dissolved oxygen. During the fermentation process, the fermentation tank needs to be kept clean and sterile because amino-acid producing cells are weak compared with wild-type strains and can be easily compromised in a contaminated environment. Moreover, the tank is controlled under positive pressure by aeration to avoid contamination by external microorganisms (Kusumoto, I., 2001). It is important to control pH, temperature, and dissolved oxygen during fermentation to achieve high yield and productivity.

Figure 1-3 illustrates the typical amino-acid crystal fermentation profile. Sugar in the medium is consumed with bacterial growth, and then it is supplied by feed medium before depletion to maintain a certain level of concentration. Subsequently, amino acids begin to accumulate in the culture broth in response to cell growth and crystallize when they reach a certain level (Patnaik, R., et al 2008, Okutani, S., et al 2012). We describe this situation as “amino acid crystal fermentation”. With increasing amino acid accumulation due to noticeable progress in fermentation process technology, the number of species of amino acid crystal fermentation has recently been increasing.

The crystal fermentation process offers both advantages and disadvantages. One advantage is that the concentration of amino acids in broth is maintained at a certain level, therefore metabolic inhibition of the target amino acid pathway and high osmolality stress can be alleviated (Cuellar, M. C., et al 2010). Another advantage is that when amino acid crystals in the broth are of high quality, the crystals can be used

directly for products (Fig. 1-4). Thus, a simplification of the downstream process of amino acid production can be achieved. On the other hand, bacterial growth is often retarded and cells are lysed during crystal fermentation because of mechanical stress of amino acid crystals on bacteria under strenuous agitation. As a result, amino acid productivity cannot achieve the expected value and impurities accumulate in the broth.

Mechanical stress caused by the presence of crystals or particles has previously been observed in the bioleaching process, in which sulfide minerals were shown to adversely affect bacterial cells (Hackl, R. P., et al 1989; Rossi, G., et al 2001). Bacterial viability is thought to be influenced by agitation speed and particle concentration, size, and shape (Deveci, H. 2002; Deveci, H. 2004). Although mechanical damage to bacterial cells has long been used as a method of cell disruption, little information is available on the process by which cells are damaged (Huff, E., et al 1964; Ananta, E., et al 2005).



(http://www.ajinomoto.com/features/amino/lets/product/shared/img/1_5_graph_02.gif)

Fig. 1-1 Schematic of production flow of L-Glutamate by fermentation

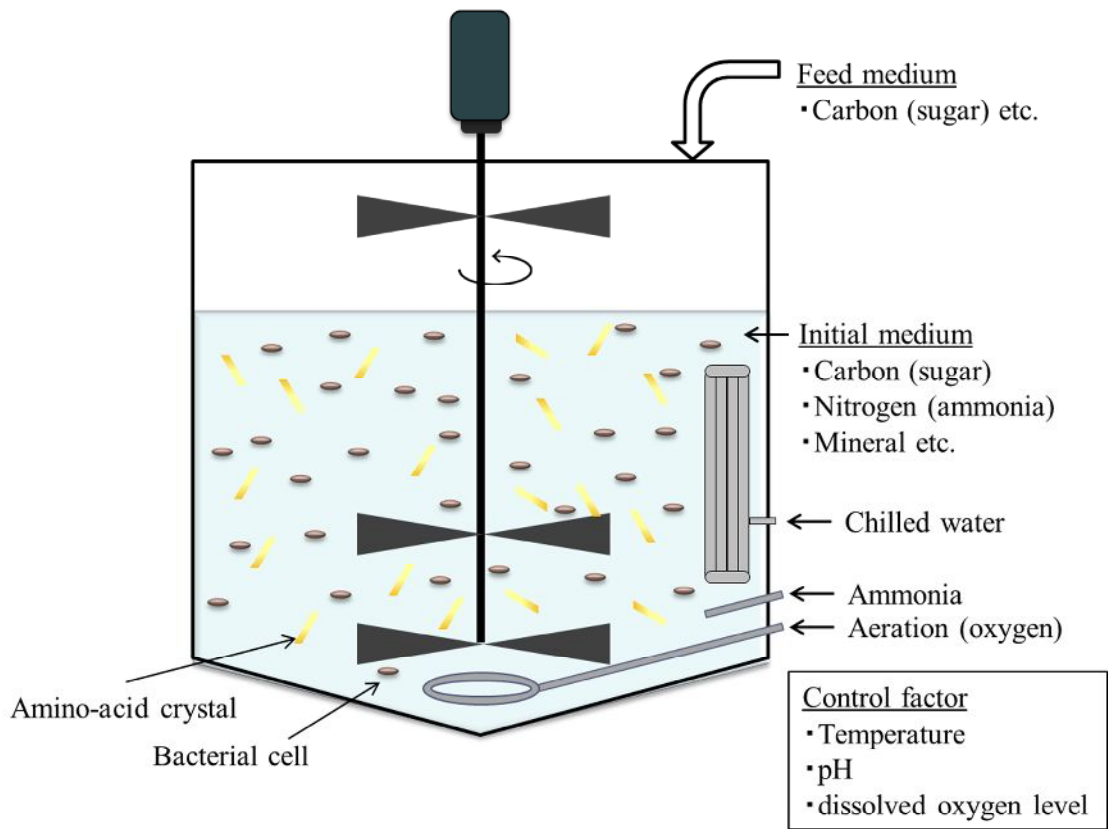


Fig. 1-2 Schematic of amino acid crystal fermentation tank

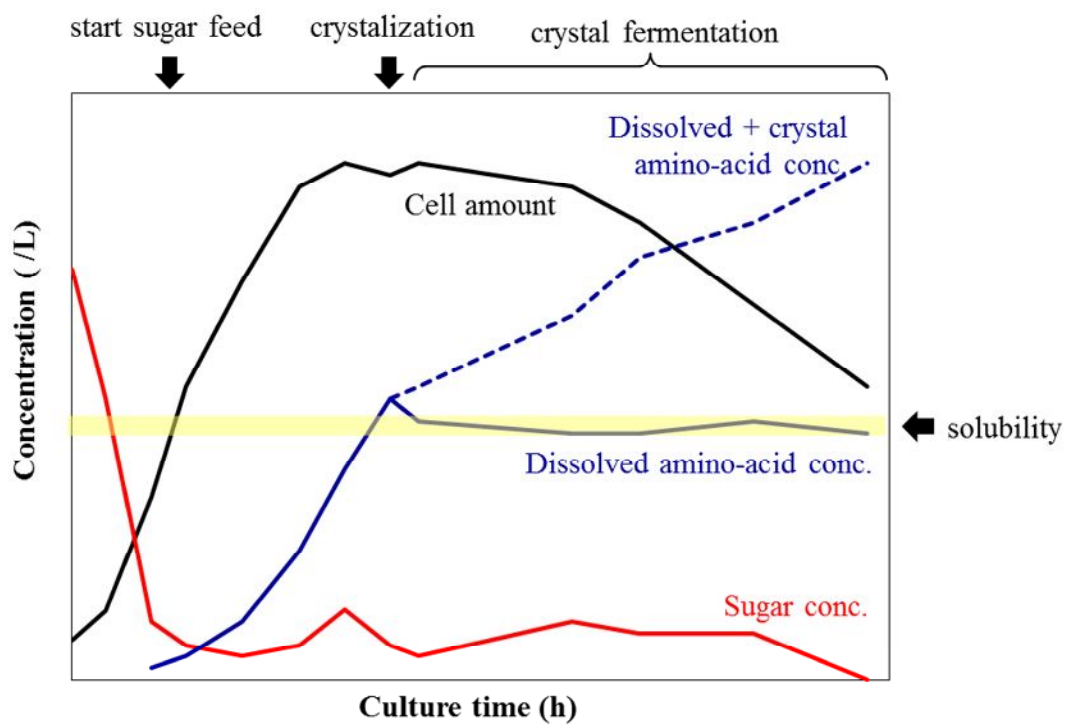


Fig. 1-3 Schematic of typical crystal fermentation profile

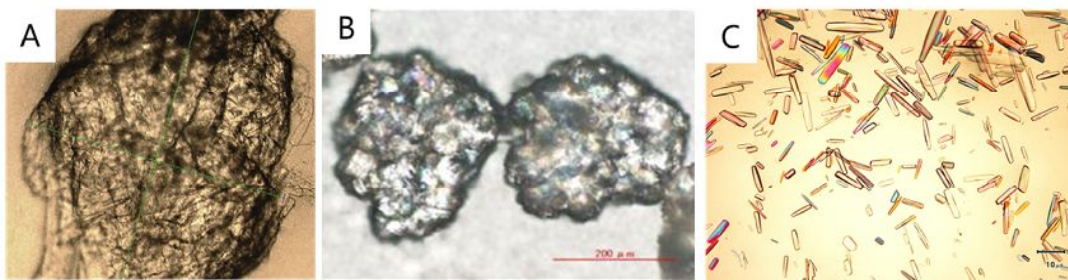


Fig. 1-4 Micrograph of amino-acid crystal from fermentation broth

(A)L-Leu crystal, (B) L-Trp crystal, (C) L-Thr crystal

Modification of culture agitation for crystal fermentation

The fundamental cause of mechanical stress might be collisions between cells and crystals. In order to decrease collision intensity and frequency, the agitation speed of the culture was reduced (Araki, M., et al 2008). We evaluated the effect of agitation speed on the mechanical stresses in L-tryptophan, L-glutamate, and L-threonine crystal fermentation processes. The bacterial cells of the amino-acid producer might be damaged by mechanical stress after crystallization.

Our results indicated that amino-acid productivities were improved at certain level by lowering agitation speed and suggested that bacterial cells were damaged by mechanical stress at higher levels of agitation speed (Fig. 1-5). The effects of the agitation speed on the productivities of crystal fermentation were different in the respective amino acids. This would be due to various reasons, e. g., the stress tolerance of each bacterial cell, the size and number of crystals, and viscosity of the media.

Lower agitation speeds, however, decreased the efficiency of oxygen dissolution in the medium. Oxygen supply to cells is one of the most critical control points for several amino acid fermentations because bacterial cells require large amounts of oxygen for growth and amino-acid production. Bacterial growth and amino acid productivity are often decreased at low levels of agitation because the availability of dissolved oxygen is limited, especially in cultivation on a commercial scale. For these reasons, this modification is not a surefire method and precise control of agitation and/or a massive amount of oxygen is required to mitigate mechanical stress in industrial applications.

With improvements in fermentation technology, the amount of crystals in the broth increases. Consequently, mechanical stress would become more serious problem.

In order for the fermentation process to be viable at an industrial level, novel methods to cope with increasing mechanical stress need to be explored.

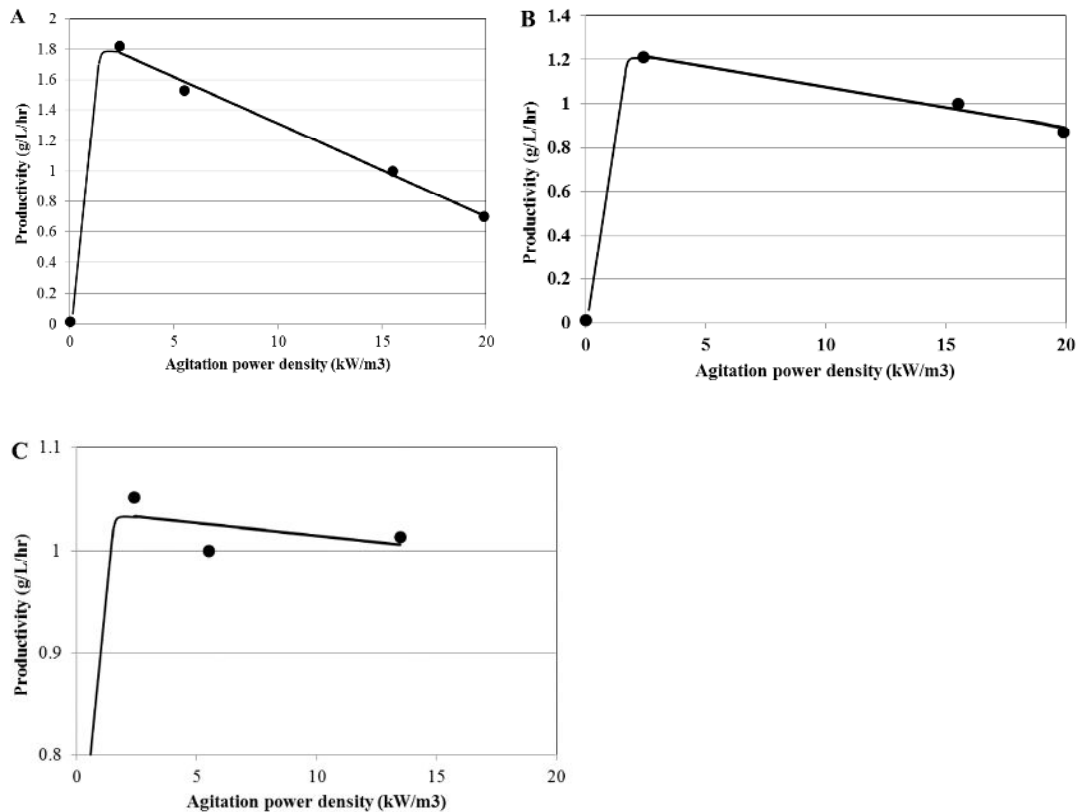


Fig. 1-5 Improvement in amino acids productivity by lower agitation speeds

(A) L-Trp fermentation was conducted under standard fed-batch flow. 10 g of Trp crystal was added to a fermenter at 23 hours of cultivation and the agitation power was changed to 2.4 kW/m³, 5.5 kW/m³, 15.5 kW/m³, and 19.9 kW/m³ during the fermentation process. Production is shown as a relative value, with the value of 15.5 kW/m³ as 1. (B) L-Glu fermentation was conducted under standard fed-batch flow. 20 g of L-Glu crystal was added to the fermenter at 23 hours of cultivation and the agitation power was changed to 2.4 kW/m³, 15.5 kW/m³, and 19.9 kW/m³ during the fermentation process. Production is shown as a relative value, with the value of 15.5 kW/m³ as 1. (C) L-Thr fermentation was conducted under standard fed-batch flow. 24 g of L-Thr crystal was added to the fermenter at 21 hours of cultivation and the agitation power was changed to 2.4 kW/m³, 5.5 kW/m³, and 13.5 kW/m³ during the fermentation process. Production is shown as a relative value, with the value of 5.5 kW/m³ as 1.

Study 1.

Mechanical stress and damage to *E. coli* cells by PVC particles

Introduction

For more than 50 years, most L-amino acids have been industrially produced by microbial fermentation from sugar sources such as glucose, sucrose, and molasses. Bacteria such as *C. glutamicum* and *E. coli* have been successfully used in the production of L-glutamic acid, L-lysine, L-threonine, L-tryptophan, L-phenylalanine, and others, which are used mainly as food ingredients, food additives, or animal feed nutrients (Hermann, T., 2003, Leuchtenberger, W., et al 2005).

The fermentation of several amino acids results in their crystallization as they accumulate above the level of their solubility (Pantnaik, R., et al 2008). This type of crystallization fermentation offers both advantages and disadvantages. Amino-acid concentrations in the fermentation broth can be maintained at low levels, and inhibition by high osmolality of dissolved product can be alleviated (Cuellar, M. C., et al 2010). The downstream process can also be simplified by using the crystals generated during fermentation to omit the crystallization step. However, bacterial cell numbers, amino-acid productivity, and yields decrease during crystallization fermentation. This appears to result from exposure of the cells to mechanical stress through mixing of the crystal-rich fermentation broth (Araki, M., et al 2008)

Mechanical stress caused by the presence of crystals or particles has previously been observed in the bioleaching processes, in which sulfide minerals were shown to adversely affect bacterial cells (Hackl, R. P., et al 1989, Rossi, G., 2001), and bacterial viability was thought to be influenced by agitation speed, particle concentration, particle size, and particle shape (Deveci, H., 2002, Deveci, H., 2004). Although mechanical damage to bacterial cells during bioreactor mixing has long been used as a method of cell disruption, little information is available on the process by which cells become

damaged (Huff, E., et al 1964, Ananta, E., et al 2005). There is thus a need to obtain basic data on the effects of mechanical stress caused by particles or crystals on bacterial cells, in order to achieve stable and high-productivity amino-acid crystal fermentation. The present study of the *E. coli* W3110 strain used polyvinyl chloride (PVC) particles as a disruptant during cultivation to examine how the cells were damaged by mechanical stress.

Materials and methods

Bacterial culture conditions

The *E. coli* W3110 strain was grown on 1.5% agar plates of LB medium containing 1.0% Bacto Tryptone (Becton Dickinson), 0.5% Bacto yeast extract (Becton Dickinson), and 1.0% sodium chloride, at 37 °C for 24 h. Approximately 10 µl (one loop) of cells was then transferred into 50 ml LB medium in a 500 ml flask and incubated at 37 °C for 7 h with shaking at 114 rpm on a rotary shaker.

Batch cultivation and fed-batch cultivation

Jar fermenters (Able Corporation) were used for both batch cultivation and fed-batch cultivation. Flask culture (100 µl) was added to 300 ml batch-cultivation medium. After complete depletion of the initial sugar from batch cultivation, 30 ml batch culture was inoculated into 300 ml fed-batch cultivation medium. These media contained 25 g/L glucose (for batch cultivation) or 30 g/L glucose (for fed-batch cultivation), 0.4 g/L MgSO₄·7H₂O, 1.0 g/L (NH₄)₂SO₄, 1.0 g/L KH₂PO₄, 0.01 g/L FeSO₄·7H₂O, 0.01 g/L MnSO₄·5H₂O, and 5.71 ml/L soybean protein hydrolysate (0.2

g/L as nitrogen). GD-113 antifoam (100 µl/L; Nof Corporation, Tokyo, Japan) was added into these media in order to suppress vigorous foaming during cultivation.

The temperature was maintained at 37 °C, and the pH was maintained at 7.0 by the addition of gaseous NH₃. Aeration was provided at 300 ml/min throughout the batch and fed-batch cultivation. Agitation was started at 800 rpm by an agitating blade, and the intensity was raised automatically to maintain a dissolved oxygen level of 5% in the cultures.

When glucose was exhausted, glucose feeding of 700 g/L was started at an appropriate rate to maintain glucose concentrations between 0 and 15 g/L during fed-batch cultivation. Cell growth was monitored by measuring OD₆₂₀ using a UV-1600 spectrometer (Shimadzu) after appropriate dilution with water. The glucose concentration of the culture supernatant was determined using a glucose analyzer BF-5 (Oji Scientific Instruments).

Cell disruption assay by PVC particles in buffer

PVC particles (Wako Pure Chemical Industries) were used to mechanically damage bacterial cells. The particles were separated based on size range into four groups, with respective average diameters of 99, 128, 153, and 163 µm, using a series of graded sieves. The sedimentation velocity of the PVC particles was significantly greater than that of bacterial cells, allowing them to be readily separated from each other.

Cell disruption by PVC particles in buffer solution was measured as follows. Cells cultivated under batch cultivation were centrifuged at 12,000 × g for 5 min at 4 °C, and the pellet was resuspended in 300 ml MES buffer (29.3 g/L 2-morpholinoethanesulfonic acid monohydrate, 8.5 g/L NaCl, pH 6.2 adjusted with

KOH). Cells were then agitated with PVC particles in the 1-L jar fermenter at 17 °C to expose them to mechanical stress.

Transmission electron microscopy (TEM) analysis

Mechanical stressed cells were fixed overnight at 4 °C in 2% glutaraldehyde and 0.1 M cacodylic acid buffer, pH 7.4, then washed four times for 15 min each in 0.1 M cacodylic acid buffer, pH 7.4, and post-fixed in 2% OsO₄ for 3 h. After three washes of 5 min each in 0.1 M cacodylic acid buffer, pH 7.4, the cells were dehydrated through an ethanol series (50–100%) for 20 min each at room temperature. The tissue was infiltrated with an epoxy resin (EPON812; TAAB Laboratories, Berkshire, UK) at 60 °C for 48 h. Ultrathin sections were counterstained with uranyl acetate and lead citrate, and examined with a JEM2000 EX transmission electron microscope (JEOL, Tokyo, Japan) (Kobae, Y., et al 2004).

Membrane-permeability analysis

Membrane-permeability analysis was performed using 2',7'-bis-(2-carboxyethyl)-5-(and-6)-carboxyfluorescein, acetoxymethyl ester (BCECF-AM; Dojindo Laboratories, Kumamoto, Japan) according to the manufacturer's method. Culture broth was diluted 100 times with water and centrifuged at 12,000 × g for 5 min at 4 °C. The supernatant was removed and the pellet was resuspended in 1 ml MOPS buffer (10 mM 3-morpholinopropanesulfonic acid, 10 mM NaCl, 130 mM KCl, 1 mM MgSO₄ at pH 6.6, 7.0, or 7.4, adjusted with NaOH). A 3 µl sample of 1 mM BCECF-AM solution was added to 1 ml suspension (final concentration, 3 µM), and incubated at 37 °C for 20 min. The mixture was then

centrifuged, and the pellet was washed twice with the same buffer. Fluorescence was measured by SpectraMAX 190 (Molecular Devices, Sunnyvale, CA) at an excitation of 500 nm, and an emission of 530 nm.

Estimation of bacterial membrane potential

Cultured bacteria were diluted with PBS buffer at pH 7.4 (137 mM NaCl, 8.1 mM Na₂HPO₄, 2.68 mM KCl, and 1.47 mM KH₂PO₄) to approximately 0.5×10^7 of bacterial cells. 3,3'- diethyloxacarbocyanine iodide (DiOC₂(3); Dojindo) was added into 200 μ l of diluted bacteria to a final concentration of 0.03 mM, and incubated for 30 min at 37 °C in the dark. Fluorescence (excitation=488 nm; emission=450 to 600 nm) was measured by a Spectra MAX M2 (Molecular Devices). The maximum fluorescent intensity between 450 nm and 600 nm wavelengths was used as the index for depolarization of membrane potential.

Determination of intracellular ATP concentration

Intracellular ATP concentrations were estimated using the BacTiter-Glo microbial cell viability assay (Promega Corporation, Madison, WI) according to the manufacturer's recommendations. Briefly, 0.1 ml culture broth or standard ATP solution (Wako Pure Chemical Industries) was mixed with 0.1 ml reagent from the assay kit. The reagent supported bacterial cell lysis and the generation of a luminescent signal that was proportional to the amount of ATP present in the bacterial cells. After mixing briefly and incubating for 5 min at room temperature, fluorescence was measured using a Spectra MAX 190 (Molecular Devices). Total ATP concentrations were determined from the

ATP standard curve and normalized by the OD₆₂₀ in order to estimate the intracellular concentrations at different stages of cultivation.

Protein analysis

The protein concentrations of the culture supernatants were assayed according to the Bradford method, using the Quick Start protein assay kit (Bio-Rad Laboratories, Hercules, CA). Bovine serum albumin (Bio-Rad Laboratories) was employed as a standard.

Results

Cell disruption assay by using PVC particles

In order to investigate the mechanical damage to *E. coli* cells, we used PVC particles as a model of amino-acid crystals. The specific gravity of the PVC particles was 1.4, which was similar to that of amino-acid crystals, but lower than those of glass beads and alumina. The use of PVC particles was therefore expected to give a similar estimate of the effect of amino-acid crystals.

We initially measured the mechanical damage to cells caused by PVC particles in buffer solution, and estimated the effects of particle concentration, agitation speed, and particle size. Cells cultivated under batch cultivation were suspended in buffer and separately agitated at 800 rpm with 60, 90, 120, or 150 g/L PVC particles (average diameter, 163 μ m). The cell lysis caused by mechanical damage, as estimated by the OD₆₂₀ and extracellular protein concentration, increased as the number of PVC particles increased (Fig. 2-1). The impact of agitation speed was then analyzed under 400, 550, 700, or 1,200 rpm agitation with 90 g/L PVC particles (average diameter, 163 μ m). As

expected, more cells were lysed as the agitation speed increased (Fig. 2-2). By contrast, particle size (average diameter, 98, 128, 153, and 163 μm) did not appear to have a significant effect on cell lysis (Fig. 2-3).

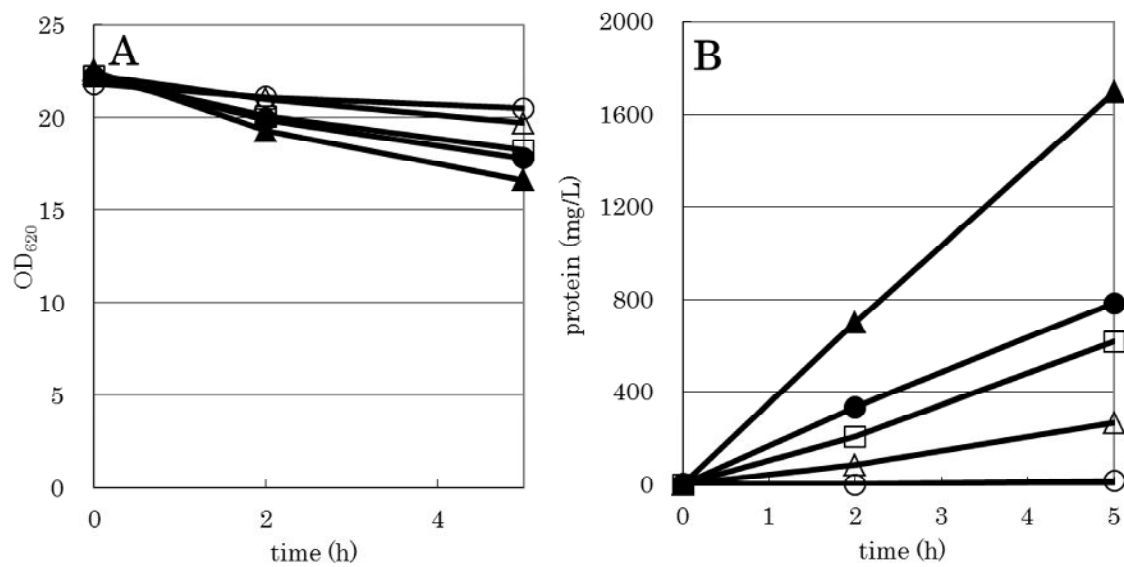


Fig. 2-1. Effect of particle concentration on *E. coli* cells by mechanical stress

Cells were agitated at 800 rpm with 0 g/L (open circles), 60 g/L (open triangles), 90 g/L (open squares), 120 g/L (closed circles), or 150 g/L (closed triangles) PVC particles (163 μm diameter) in buffer solution. Cell disruption was evaluated by (A) OD₆₂₀ and (B) extracellular protein concentration.

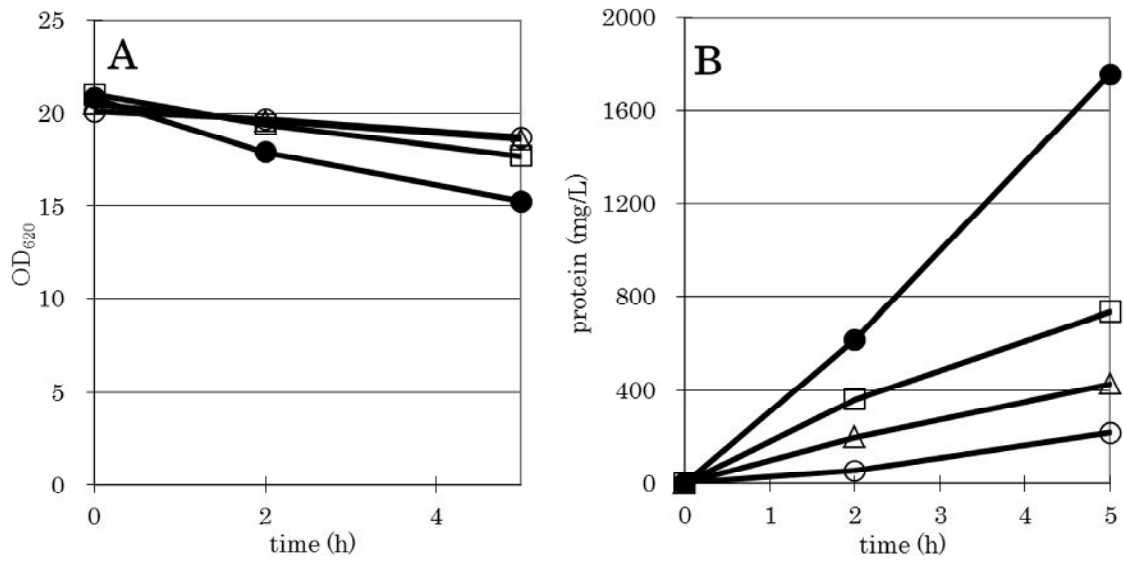


Fig. 2-2. Effect of agitation speed on *E. coli* cells by mechanical stress

Cells were agitated at 400 rpm (open circles), 550 rpm (open triangles), 700 rpm (open squares), or 1,200 rpm (closed circles) with 90 g/L PVC particles (163 μ m diameter) in buffer solution. Cell disruption was evaluated by (A) OD₆₂₀ and (B) extracellular protein concentration.

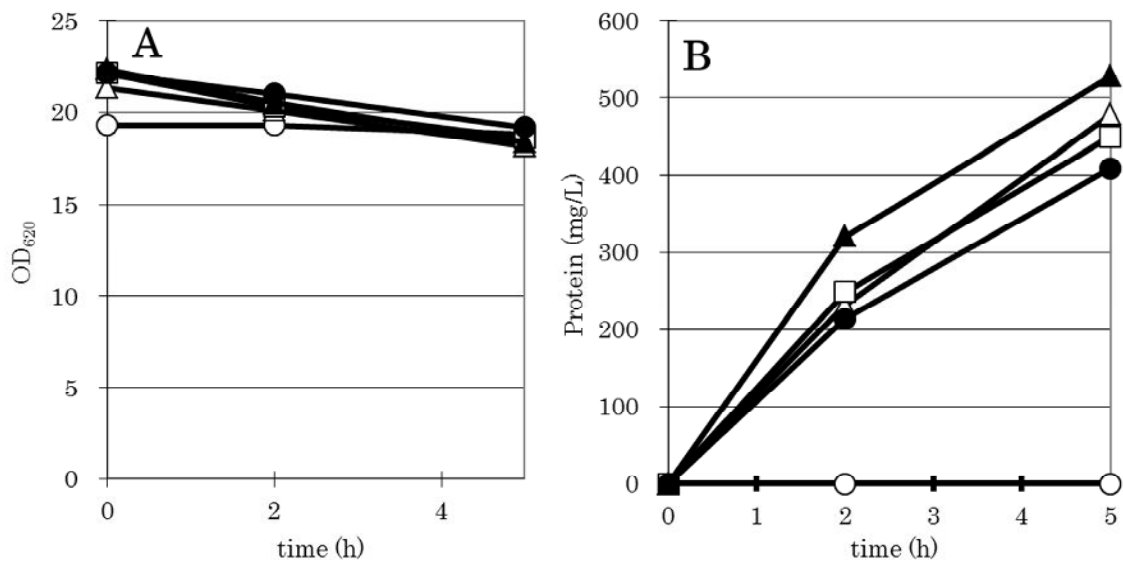


Fig. 2-3. Effect of particle size on *E. coli* cells by mechanical stress

Cells were agitated at 800 rpm without particles (open circles), or with 99 μ m (open triangles), 128 μ m (open squares), 153 μ m (closed circles), or 163 μ m (closed triangles) diameter PVC particles in buffer solution. Cell disruption was evaluated by (A) OD₆₂₀ and (B) extracellular protein concentration.

Next, we examined the mechanical stress to cells caused by PVC particles during fed-batch cultivation, in order to study the bacterial response to mechanical stress. In this experiment, 0, 30, 60, and 90 g/L PVC particles (average diameter; 128 μm) was added to the jar fermenter at a culture time of 20 hours during the fed-batch cultivation. The agitation speed was maintained at a constant rate of 800 rpm, which is sufficient to maintain 5% dissolved oxygen, after 20 hours. Cell lysis increased after the addition of PVC particles, and the response was dependent upon the particle concentration (Fig. 2-4). PVC particle addition caused severe cell damage, resulting in cell disruption and the formation of pores in the cell membrane (Fig. 2-5). The specific glucose consumption rate, measured as the consumed glucose weight per dry cell weight per h, was temporarily increased after the addition of PVC particles; in particular, the ν value increased more than twofold in the presence of 90 g/L PVC particles (Fig. 2-4 (C)). The specific glucose consumption rate value decreased after 30 h of cultivation with 90 g/L particles. These results showed that high mechanical stress temporarily increased the glucose consumption by the cells, which subsequently fell.

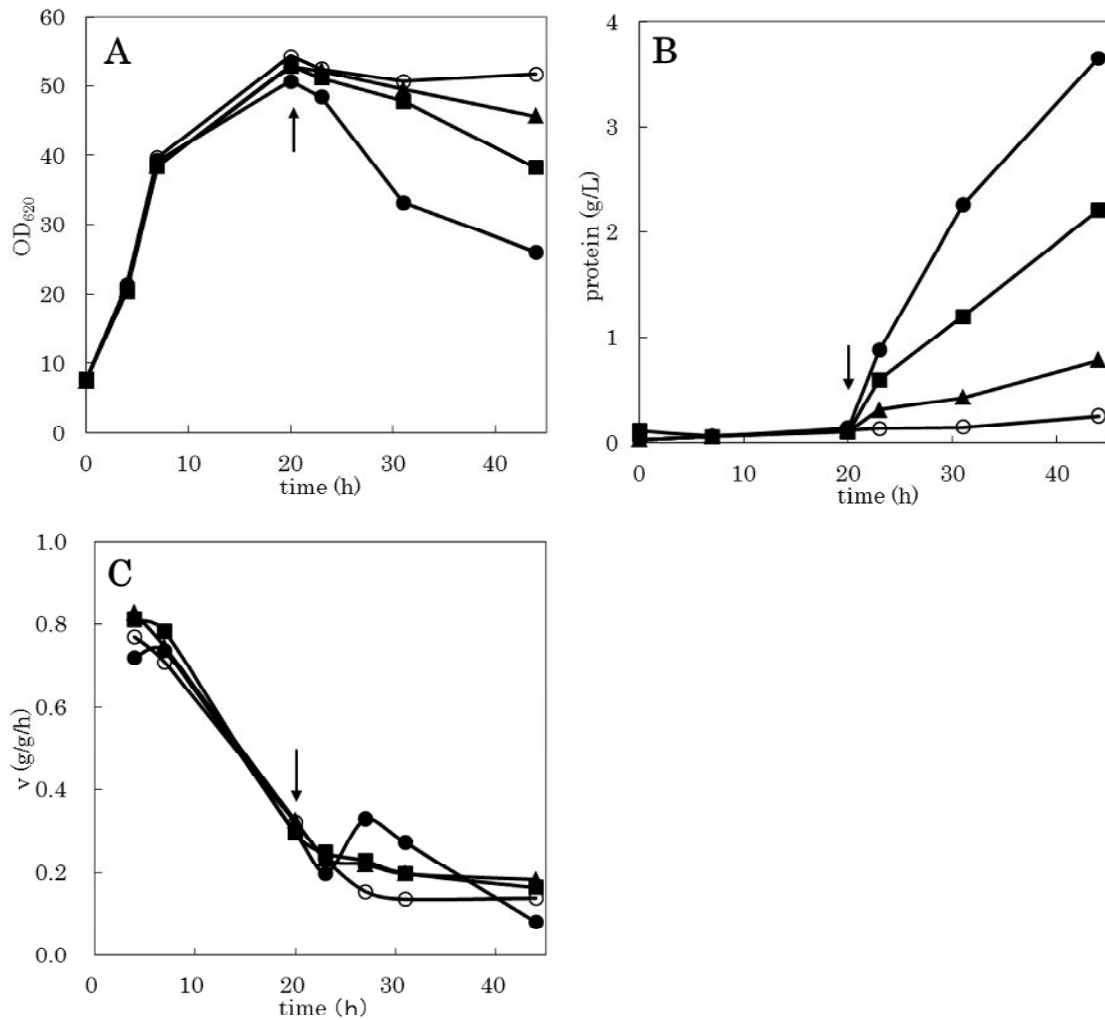


Fig. 2-4 Mechanical damage to *E. coli* cells under fed-batch cultivations

In this cultivation, 0 g/L (open circle), 30 g/L (closed triangle), 60 g/L (closed square), or 90 g/L (closed circle) PVC particles (128 μm diameter) were added to the jar fermenter at CT 20 h (arrow) during fed-batch cultivation. Cell disruption was evaluated by (A) OD₆₂₀ and (B) extracellular protein concentration. (C) The specific glucose consumption rates (ν) were calculated as the consumed glucose weight per dry cell weight per hours.

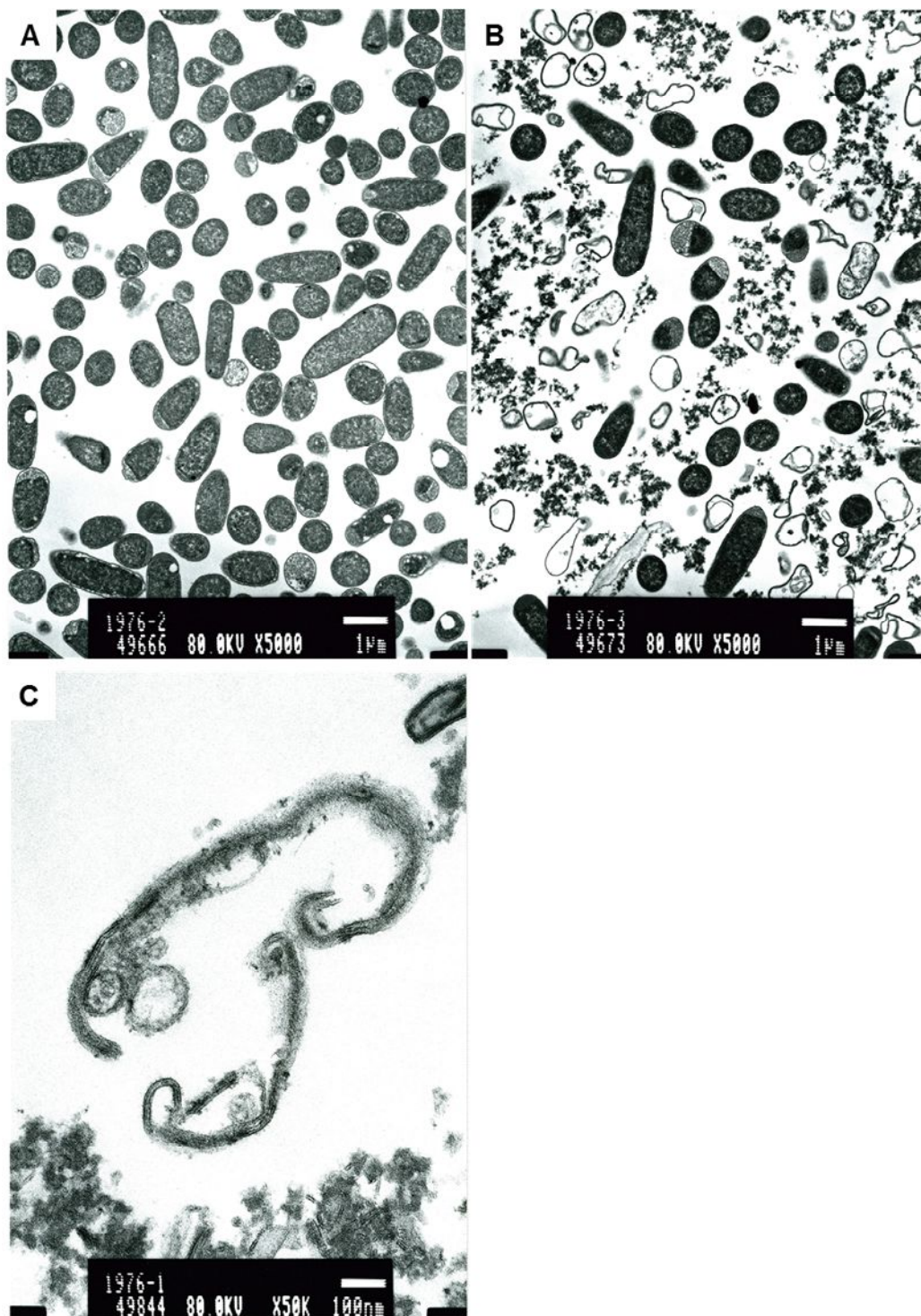


Fig. 2-5 Electron micrograph of *E. coli* cells with mechanical stress

E. coli cells grown under fed-batch cultivation conducted (A) without, or (B) and (C) with 90 g/L PVC particles (128 μm diameter) at CT 20 h. (A) and (B) scale bar, 1 μm ; (C) scale bar, 100 nm.

Membrane permeability and intracellular homeostasis of damaged cells

In order to evaluate the membrane damage caused by mechanical stress under fed-batch cultivation, we estimated the membrane permeability after the addition of PVC particles using the pH-sensitive fluorescent dye BCECF-AM, which has a pH-dependent fluorescence-excitation profile (Rink, T. J., et al 1982; van Veen, H. W., et al 1994; Glaasker, E., et al 1996). Once inside the cell, BCECF-AM is cleaved by non-specific esterase, resulting in a charged form of BCECF that leaks out of cells more slowly than its parental compound (Volk, C., et al 1998).

The internal pH of bacterial cells is reported to maintain between 7.4 and 7.8 irrespective of culture pH (Slonczewski, J. L., et al 1981; Zilberstein, D., et al 1984). The internal pH of the cells challenged by mechanical stress was expected to change in response to the external pH. This was confirmed with following experiments. The membrane permeability of the damaged cells in the fed-batch cultivation with 90 g/L PVC particles at CT 20 h was evaluated by re-suspending the cells in MOPS buffer at pH 7.4, 7.0, and 6.6 with BCECF-AM. The fluorescence level of the damaged cells was found to become higher in a time-dependent manner than that of normal cells (Fig. 2-6), indicating that dye permeability was increased by the mechanical damage caused by PVC particles. The fluorescence level of the damaged cells was also shown to increase as the pH of the external buffer increased. Damaged bacteria are thought to demonstrate changes in cell surface properties and structure, and to be subject to adverse effects on osmoregulation, enzyme activity, protein synthesis, and cell division (Tsuchido, T., et al 1985).

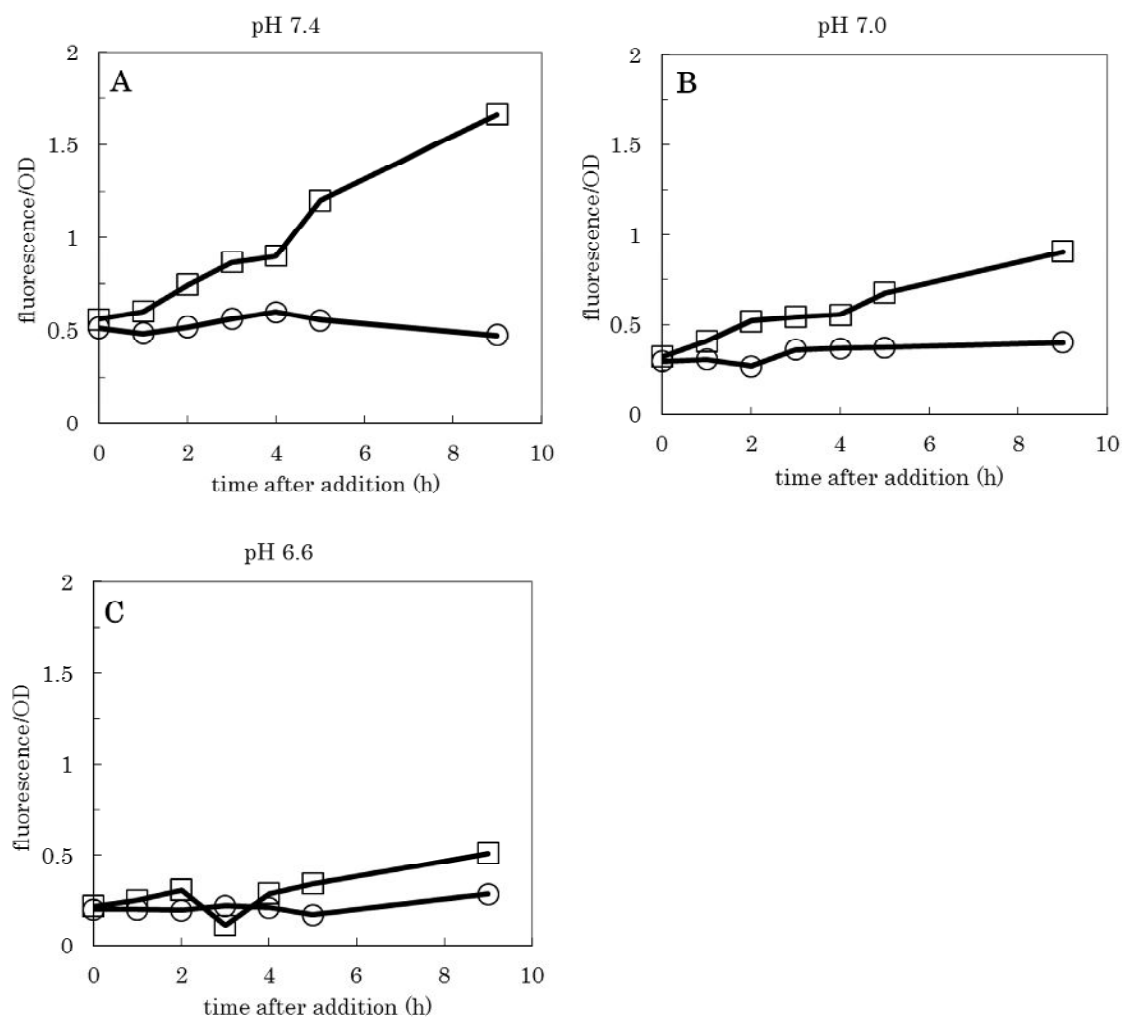


Fig. 2-6 BCECF-AM fluorescence in mechanical stressed *E. coli* cells

Fluorescence of non-damaged cells without 90 g/L PVC particles (circles) or damaged cells with 90 g/L PVC particles (squares) analyzed at (A) pH 7.4, (B) pH 7.0, or (C) pH 6.6.

Bacterial membrane potential

Bacterial membrane potentials are thought to decrease under the mechanical stress condition due to the considerable damage to bacterial membrane structures. Bacterial membrane potentials were estimated using the membrane-potential-sensitive fluorescent dye DiOC₂(3), which changes its cellular location and fluorescent intensity according to the membrane potential (Fig. 2-7 (A)).

The membrane potentials of bacteria under the stress were measured in fed-batch cultivation of *E. coli* cells. 90 g/L of PVC crystal was added at 20 h of cultivation, at agitation speeds of 1,000 rpm or 1,500 rpm. The number of bacteria calculated by OD₆₂₀ was found to decrease and the extracellular protein concentrations increased with increasing agitation speeds (Fig. 2-7 (B), (C)). The bacterial membrane potentials, as estimated by DiOC₂(3) fluorescent intensity, were found to increase in proportion to the number of crystals and agitation speed (Fig. 2-7(D)). Bacterial membrane potential tends to be depolarized drastically when above a certain level of mechanical stress.

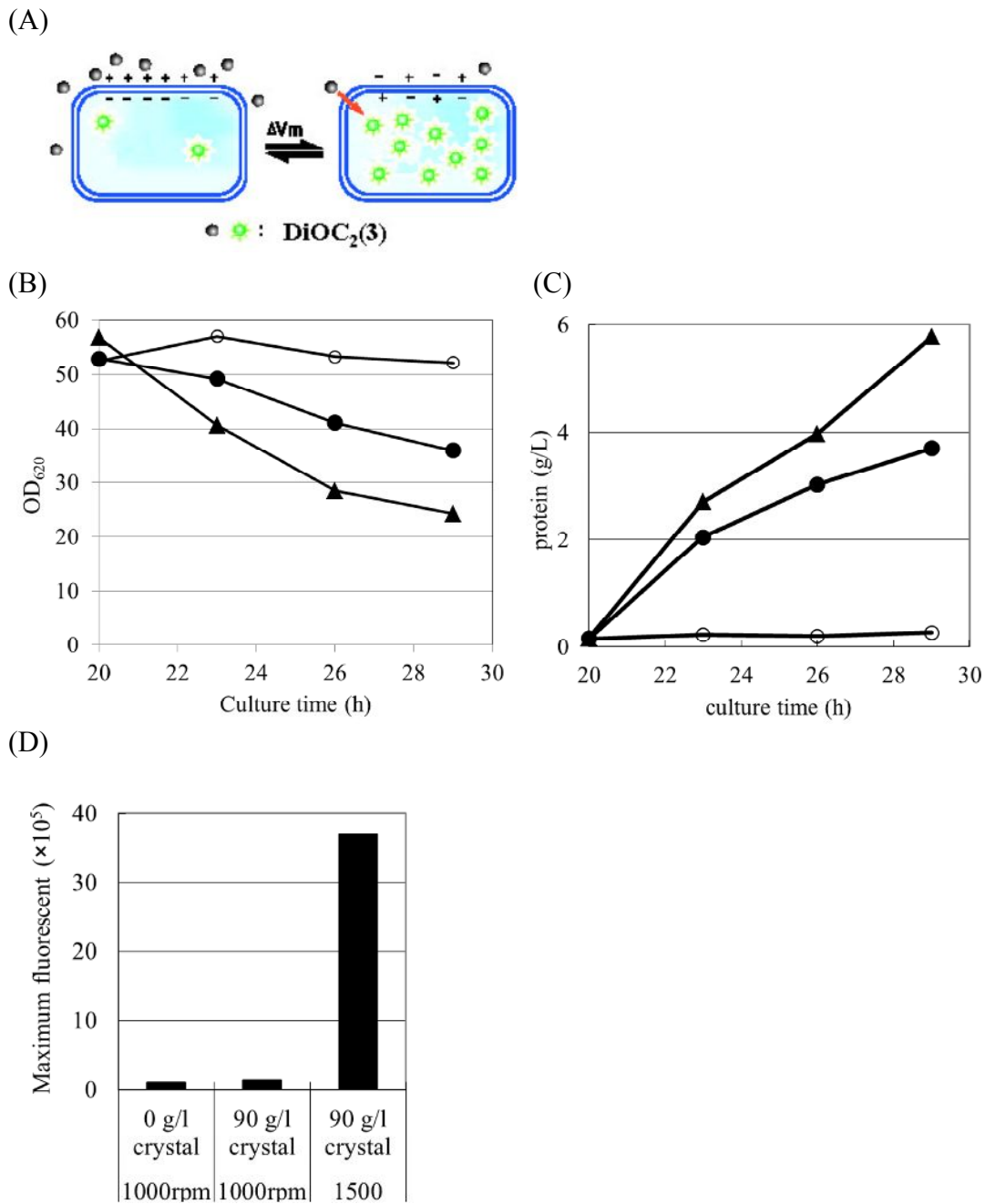


Fig. 2-7 Estimation of the membrane potential in *E. coli* cells with the stress

(A) Measurement principle of membrane potential using DiOC₂(3) (revised “Instruction “of Dojindo)

(B) OD₆₂₀ profile and (C) extracellular protein concentration after addition of PVC particles at 20 h in fed-batch cultivation of *E. coli* cells. Fed-batch cultivation was conducted with 0 g/l crystal at 1,000 rpm (open circle), 90 g/l crystal and 1,000 rpm (closed circle), 90 g/l crystal and 1,500 rpm (closed triangle).

(D) Bacterial membrane potential depolarization of 6 h after crystal addition, as shown by DiOC₂(3) fluorescent intensity .

Intracellular ATP concentration

The intracellular ATP concentrations of mechanically damaged cells were examined using the BacTiter-Glo microbial cell viability assay (Promega). The ATP levels of damaged cells cultivated under fed-batch cultivation were measured sequentially over time following the addition of 90 g/L PVC particles at CT 20 h.

The ATP concentrations were temporarily increased during the first 7 h after the addition of PVC particles, and subsequently started to decrease (Fig. 2-8). The timing of the ATP level rise coincided with that of the activation of the v , resulting in the enhancement of the glycolytic system (Fig. 2-4 (C)). The decrease in ATP levels was likely to have resulted from the considerable damage done to the cell membrane.

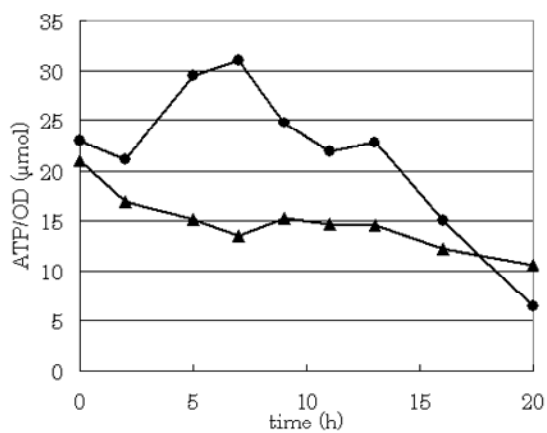


Fig. 2-8 Intracellular ATP levels of *E. coli* cells grown under fed-batch cultivation

Non-damaged cells (triangles) and damaged cells (circles) were prepared from fed-batch cultivation with or without 90 g/L PVC particles (128 μm diameter) at CT 20 h. Intracellular ATP levels were estimated using the BacTiter-Glo microbial cell viability assay sequentially over the following CT 20 h.

Discussion

Fermentation production results in the crystallization of several types of amino acid. The bacterial cell numbers and amino-acid yields are known to decrease during this process. This study investigated the mechanical stress to the *E. coli* W3110 strain caused by PVC particles, and the resulting cell disruption. We also attempted to find a means to alleviate the mechanical stress and cell lysis.

We initially evaluated bacterial cell suspensions in buffer with PVC particles, in order to examine the mechanical damage to non-growing cells. The cell lysis increased in proportion to the number of particles and the agitation speed; this suggested that the degree of mechanical damage and cell disruption were correlated with the number of collisions between cells and PVC particles by vigorous agitation. Growing cells under fed-batch cultivation suffered similar damage caused by PVC particles. The frequency of cell disruption was again increased when more particles were used.

The improvement of glucose-consumption activity was observed several hours after the addition of PVC particles under fed-batch cultivation, and was correlated with an increase in intracellular ATP concentration. As mechanical damage induces increased membrane permeability, glucose might be taken up by the cells through the damaged membrane in addition to the normal phosphotransferase system. The uptake of glucose through the membrane is one of the rate-determining steps of glucose consumption. If the cells maintain a sufficient level of enzymes in the glycolytic pathway in which substrate phosphorylation occurs, the ATP production by substrate phosphorylation can be temporarily enhanced until the cells are severely damaged.

The bacterial membrane potential tended to depolarize under the mechanical stress condition because the cellular membrane might be broken and opened pore by the

damage. The damaged membrane might be unable to maintain a proton gradient, resulting in decreased ATP production activity using oxidative phosphorylation, similar to the depolarization response induced by uncouplers (Reider, E., et al 1979). This could have a negative effect on ATP production in damaged cells. A transiently elevated and subsequently downturned intracellular ATP-concentration profile could be observed as the result of a balance between the improved glucose uptake following substrate phosphorylation and the decline in the proton gradient resulting from membrane damage.

Our model of response to the mechanical stress caused by PVC particles to *E. coli* cells is summarized in Fig. 2-8. Mechanisms to alleviate mechanical stress during amino acid crystal fermentation are thought to exist in bacterial cells. Further detailed studies, involving transcriptome analysis and the investigation of membrane structural changes, will be undertaken to elucidate the mechanisms of the mechanical damage and to construct a strategy for alleviating such stress.

Mechanical stress by PVC particle

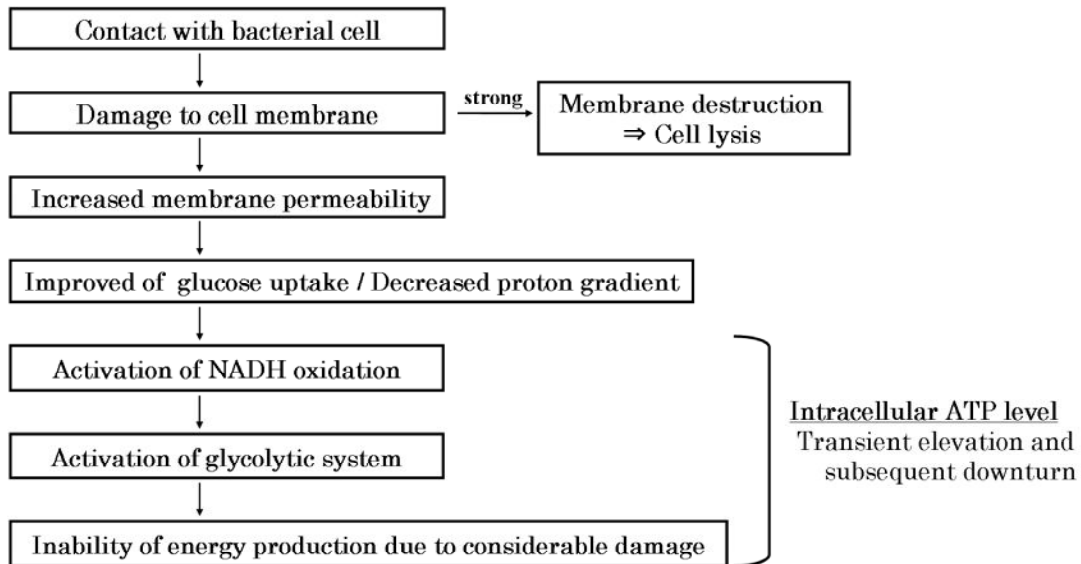


Fig. 2-8 Diagram of mechanical stress caused by PVC particles.

Mechanical damage due to contact between bacterial cells and PVC particles is the main trigger of mechanical stress. Excess damage induces bacterial membrane destruction and cell lysis. Mechanical damage to bacterial membranes increases membrane permeability, concurrent with increases in glucose uptake (v) and decreases of the proton gradient across the membrane. The decreases of proton gradient were alleviated by activation of NADH oxidation to produce ATP by oxidative phosphorylation and subsequently activation of the glycolytic system to supply NADH and ATP. Intracellular ATP concentrations were transiently elevated and subsequently decreased, which is determined by the balance of glycolytic system, NADH oxidation, and oxidative phosphorylation on the membrane. Finally, the cells couldn't produce energy due to the considerable damage of membrane stress by PVC particles.

Study 2.
Fe-S cluster assembly machinery responsible
for relief of the mechanical stress

Introduction

For more than 50 years, most L-amino acids have been industrially produced from sugar sources, such as glucose, sucrose, or molasses by fermentation technology of microorganisms. Bacterial strains derived from *C. glutamicum* and *E. coli* have been successfully developed for the production of L-glutamic acid, L-lysine, L-threonine, L-tryptophan, L-phenylalanine, and others, which are mainly used as food ingredients, food additives, or animal feed nutrient (Thomas, H., 2003, Leuchtenberger, W., et al 2005). Some amino acids secreted into culture broth from bacterial cells accumulate to a level exceeding their solubility and result in crystallization (Patnaik, R., et al 2008). This type of crystal fermentation offers two advantageous situations. First, product inhibition of metabolic pathway of the amino-acid fermentation can be alleviated (Cuellar, M. C., et al 2010), because the concentration of amino acids in broth is maintained at a certain level. Second, a direct use of crystals of amino acids collected from broth simplifies processes of amino-acid production.

Growth of bacterial cells, however, is often retarded or is stopped during the crystal fermentation, because crystals of amino acids give a mechanical stress to bacterial cells. As a result, amino-acid production yield is decreased, and compounds other than amino acids are accumulated to inhibit bacterial growth. There are two strategies proposed to avoid these negative effects. One is development of culture system for reduction of mechanical stress (Araki, M., et al 2012) and the other is generation of mechanical stress tolerant cells. The mechanical stress caused by the combination of agitation and solid crystal particles can be alleviated by lowering agitation speed. However, subtle controls of agitation and aeration are required to avoid

growth retardation of bacterial cells and this would give a restraint to achieve stable amino-acid crystal fermentation, in particular, fed-batch cultivation of industrial scale. Bacteria seem to have physiological potential to cope with mechanical stress and detailed studies of bacterial response to mechanical stress would be of importance for invention of a new strategy for alleviating such stress. We previously investigated mechanical damage of *E. coli* cells caused by an addition of PVC particles into culture medium and proposed that this experimental system was applicable as a model of amino-acid crystal fermentation (Okutani, S., et al 2012). The particles with a diameter of around 100 μm had a specific gravity and surface properties similar to most amino-acid crystals. Responses of bacterial cells to the PVC particle stress seemed to mimic phenomena occurred in the actual crystal fermentation. The addition of PVC particles lowered integrity of the cell membrane and caused change of its permeability. A temporal increase in both glucose consumption and intracellular ATP concentration was induced before bacterial cells were severely damaged. These observations suggested that glycolytic pathway was enhanced in response to the mechanical stress (Okutani, S., et al 2012).

It is worthwhile to notice that ROS induced by the mechanical stress inactivates enzymes containing Fe-S cluster vulnerable to oxidative stress (Johnson, D. C., et al 2005), and thus that cellular ability of the Fe-S cluster assembly might be elevated to retain activity of Fe-S cluster-containing enzymes functioning in the energy-releasing pathways of the glucose consumption.

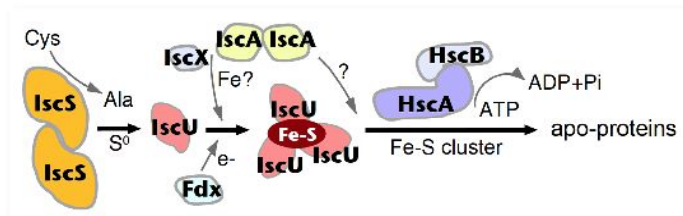
E. coli possesses two Fe-S cluster assembly machineries, termed ISC and SUF systems encoded by the *isc* (*iscRSUA-hscBA-fdx-iscX*) and *suf* (*sufABCDSE*) operons, respectively (Johnson, D. C., et al 2005, Ayala-Castro, C., et al 2008, Fontecay, M., et

al 2008, Tokumoto, U., and Takahashi, Y. 2001, Takahashi, Y., and Tokumoto, U. 2002). Both systems are responsible for the maturation of a wide variety of Fe-S proteins without strict specificity for apo-protein targets or Fe-S cluster types (either [2Fe-2S], [4Fe-4S] or [3Fe-4S]) (Fig. 3-1) (Tokumoto, U., et al 2004). The ISC machinery functions as a major assembly pathway in normal growth conditions, whereas SUF machinery plays a role in Fe-S cluster biosynthesis under adverse conditions such as oxidative stress and iron starvation (Fontecav, M., et al 2008). The ISC and SUF systems share similarity in their requirement for a cysteine desulfurase (IscS and SufS) that functions as a sulfur donor (Johnson, D. C., et al 2005, Ollagnier-de-Choudens, S., et al 2004, Lu, J., et al 2008). Among these components, IscU and SufBCD complex, called scaffold proteins, are responsible for de novo Fe-S cluster assembly. IscU accepts sulfur and iron atoms, and promotes the assembly of Fe-S cluster (Agar, J. N., et al 2000, Smith, A. D., et al 2001). HscA and HscB synergistically interact with IscU and facilitate Fe-S cluster release from IscU for the transfer to apo-protein targets (Hoff, K. G., et al 2000, Hoff, K. G., et al 2003, Chandramouli, K., and Johnson, M. K. 2006, Vickery, L. E., and Cupp-Vickery, J. R. 2007).

In this report, the expression of various components involved in Fe-S cluster assembly was investigated in *E. coli* cells growing under the mechanical stress of PVC particles. The level of HscA was found to increase significantly with appearance of a new molecular form, while most of other components of the Fe-S cluster assembly machinery showed no significant changes. The cellular activity of Fe-S cluster-containing enzymes was decreased under the mechanical stress and an overexpression of HscA could alleviate this decrease. We think that *E. coli* copes with the mechanical

stress by increasing expression level of HscA and propose that this phenomenon could apply for an improvement of the amino-acid crystal fermentation.

(A)



(B)

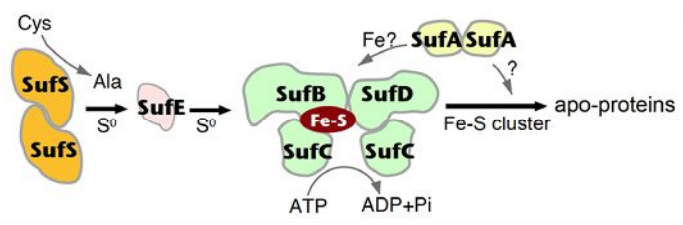


Fig. 3-1 Schematic of Fe-S cluster assembly systems (A) ISC machinery, (B) SUF machinery

Materials and methods

Bacterial strain and culture conditions

The *E. coli* W3110 strain was used in this study. Bacterial cells were streaked on 1.5% agar plates of LB medium containing 1.0% Bacto tryptone (Becton Dickinson), 0.5% Bacto yeast extract (Becton Dickinson), and 1.0% sodium chloride and grown at 37 °C for 24 hours. Approximately 10 µl of the cells was transferred into 50 ml LB medium in a 500 ml flask. The flask culture was incubated at 37 °C for 15 hours with shaking at 114 rpm on a rotary shaker.

Fed-batch cultivation

One-L jar fermenter (Able Corporation) was used for fed-batch cultivation. The abovementioned flask culture was inoculated into 300 ml of fed-batch culture medium. This medium contained 30 g/L glucose, 0.4 g/L MgSO₄·7H₂O, 1.0 g/L (NH₄)₂SO₄, 1.0 g/L KH₂PO₄, 0.01 g/L FeSO₄·7H₂O, 0.01 g/L MnSO₄·5H₂O, and 5.7 ml/L soybean protein hydrolysate (0.2 g/L as nitrogen). The bacterial cells were grown at 37 °C under stirring agitating blade at 1000 rpm with aeration at 300 ml/min, and pH of the medium was maintained at 7.0 by adding gaseous NH₃ throughout the cultivation. One hundred µl/L of antifoam, GD-113 (Nof Corporation), was added to avoid vigorous foaming during cultivation.

The glucose concentration of the medium was monitored by using glucose analyzer BF-5 (Osi Scientific Instruments) and the concentration was maintained between 2 to 30 g/L by a continuous feeding of 700 g/L glucose. Cell growth was monitored by measuring OD₆₂₀ using UV-1600 spectrometer (Shimadzu, Japan) after an appropriate dilution.

PVC particles (Wako Pure Chemical Industries) with an average diameter of 128 μm were added into the medium to final concentrations from 0 g/L to 100 g/L to subject the bacterial cells to mechanical stress. PVC particles were easily removed from the bacteria culture by sedimentation.

Protein analysis

Protein concentration was determined by Bradford method, using the Quick start protein assay kit (Bio-Rad laboratories, USA). Bovine serum albumin (Bio-Rad laboratories) was employed as a standard.

Enzyme assays

Bacterial cells were harvested by centrifugation and washed with 50 mM Tris-HCl, pH 7.5 containing 150 mM NaCl and 0.6 mM MnCl_2 . Cell-free extracts were obtained by sonication followed by centrifugation at 15000 rpm for 10 min.

Aconitase activity was assayed in a 1.0-ml reaction mixture containing 50 mM Tris-HCl, pH 7.4, 30 mM sodium citrate, 0.6 mM MnCl_2 , 0.2 mM NADP^+ , 2 units/ml of isocitrate dehydrogenase, and an appropriate amount of cell-free extracts, and then formation of NADPH was monitored at 37°C by following absorbance at 340 nm (Gardner, P. R., and Fridovich I. 1992). Succinate dehydrogenase activity was measured by the phenazine methosulfate (PMS) coupled reduction of 3-(4,5-dimethylthiazolyl-2)-2,5-diphenyltetrazolium bromide (MTT) (Futai, M., 1973). The reaction mixture contained 80 mM Tris-HCl, pH 7.5, 60 μM of MTT, 120 μM of PMS, 10 mM of sodium succinate, 0.1% (w/v) Triton X-100, and an appropriate amount of the cell-free extracts, and the increase of absorbance at 570 nm was followed at 25°C.

Malate dehydrogenase activity was assayed in a 0.2 ml reaction mixture containing 50 mM Tris-HCl, pH 7.5, 0.5 mM oxaloacetate, and 2 mM NADH, and oxidation of NADH was monitored at 30°C by following absorbance at 340 nm.

Micro-tube treatment for mechanical stress

The *E. coli* cell was grown on 1.5% agar plates of LB medium containing 1.0% Bacto Tryptone (Becton Dickinson, Franklin Lakes, NJ), 0.5% Bacto yeast extract (Becton Dickinson), and 1.0% sodium chloride, at 37 °C for 24 h. Appropriate amount of the cell was suspended with 50 mM phosphate buffer solution. Bacterial suspension of 1.0 ml was transferred to 1.5 ml micro-tube with 0.1 g PVC crystals and 2 mg glucose. This micro-tube was set to TissueLyser (Qiagen) and shake vigorously by 30 times/s for one hour.

Measurement of superoxide anion and hydrogen peroxide

Superoxide anion (O_2^-) was detected using water-soluble tetrazolium salts WST-1 (4-[3-(4-iodophenyl)-2-(4-nitrophenyl)-2H-5-tetrazolio]-1,3-benzene disulfonate sodium salt). WST-1 can be reduced by superoxide anion selectively and forms formazan having an absorption maximum at 438 nm (Ukeda, H., et al 2002). 100 μ M of the WST-1 was added into micro-tube assay system and subsequently measured absorption wavelength 438 nm of the supernatant. Generation of superoxide anion was calculated molar adsorption coefficient of the formazan at 11 /mM/cm.

Hydrogen peroxide (H_2O_2) in the supernatant of micro-tube assay system was measured using Amplex Red Hydrogen Peroxide/Peroxidase Assay kit (Invitrogen, Carlsbad, CA) according to the manual.

Analysis of gene expression using DNA microarray

E. coli cells were grown in a fed-batch culture for 20 h and then further cultivated after addition of 100 g/L of PVC particles. The cells cultivated in the presence or absence of PVC particles were harvested at 9 h and 21 h and the cells were subjected to preparation of the total RNAs. Total RNA samples from *E. coli* cells were obtained using the RNeasy Protect Bacteria Mini Kit (Qiagen, Venlo, Netherlands) according to the manufacturer's recommendation.

The *E. coli* DNA microarrays for gene expression analysis were designed to contain 24-mer probes on NimbleGen 1x385K arrays (Roche NimbleGen, Inc. Madison, WI). Oligonucleotide array comparative genomic hybridization was carried out by NimbleGen Systems (Roche NimbleGen) according to previously published methods for DNA labeling, array construction and hybridization. cDNA was synthesized by SuperScriptRII RNase H-Reverse Transcriptase (Invitrogen) from 10µg of total RNA and Random Primer (Invitrogen).

Following RNA degradation by RNase H (Invitrogen) and RNase A (promega, Fitchburg, WI), the cDNA was purified by 25:24:1 of phenol:chloroform:isoamyl alcohol, which saturated with 10 mM Tris-HCl (pH 8.0) and 1 mM EDTA, and ethanol precipitation. The cDNA was digested with DNase I (Promega) to obtain from 50 to 200-bp fragments and the fragments were labeled by using terminal Deoxynucleotidyl transferase and biotin-N6-ddATP (PerkinElmer, Inc., Winter Street Waltham, MA). Millipore Microcon Centrifugal Filter Devices, YM-10 (Millipore, Billerica, MA) were used to remove free biotin-N6-ddATP from the transferase reaction mixtures. Microarray hybridization experiments were performed using Nimblegen standard

protocol as follows. The labeled cDNA samples were hybridized to arrays for 16 to 20 h at 45°C. Following hybridization, samples were washed and a streptavidin-Cy3 conjugate was used to stain each microarray. The arrays were scanned by using an Axon GenePix 4000B scanner (Molecular Devices) with the GenePix Pro software (Molecular Devices). Signal intensity data were extracted from obtained images by using the NimbleScan software.

Western blotting

Expression levels of Fe-S cluster assembly machinery components were analyzed by SDS-PAGE followed by Western blotting (Onda, Y., et al 2000). The bacterial cells were sonicated in buffer W (50 mM Tris-HCl, pH 7.5 and 150 mM NaCl) on ice for 2 min and centrifuged at $15,000 \times g$ for 10 min at 4°C. The supernatant was separated by SDS-PAGE, electroblotted to a polyvinylidene difluoride membrane (Merck Millipore, Darmstadt, Germany), and decorated with rabbit antibodies raised against either HscA, HscB, IscA, IscR, SufA, or SufB (Takahashi, Y., and Tokumoto, U. 2002, Tokumoto, U., 2004). Rabbit antibodies against DnaK were purchased (Enzo Life Sciences, USA). The antigen-antibody complex was visualized by reaction with alkaline phosphatase conjugated goat antibodies against rabbit IgG (Bio-Rad).

Construction of HscA expression plasmids

The *hscA* gene was amplified by PCR from *E. coli* genome using TaKaRa Ex Taq polymerase (Takara Bio Inc. Shiga, Japan), forward primer (GGTACCTCGATTTTAAATTTCTGGAAG, *KpnI* site underlined) and reverse primer (GTCGACTATTAAACCTCGTCCACGGAATG, *SalI* site underlined), and cloned into

the pCR2.1-TOPO vector (Invitrogen) by the TA cloning method. The *KpnI-SalI* fragment was excised and cloned into the pBBR1MCS-4 vector (Kovach, M. E., et al 1995). HscA was expressed under the control of the lac promoter in the presence of 0.1 mM isopropyl β -D-1-thiogalactopyranoside (IPTG). HscA was tagged with hexahistidine sequence at the C-terminus by inverse PCR from the pBBR1MCS-4-*hscA* plasmid using primers GCCAACCTCGTCCACGGAATGGC and CACCACCACCACCACCCTGAGCTCCAATTCGCCCTATAGTG, followed by *DpnI* treatment, 5' terminal phosphorylation, and self-ligation. Construction of the N-terminal hexahistidine-tagged HscA was described previously (Tokumoto, U., et al 2002).

To induce *hscA* gene in pBBR vector, IPTG was added to a final concentration of 0.1 mM in the culture.

Interaction of his-tag HscA with Ni column

Appropriate amount of cell pellets were resuspended in 200 ml buffer W and disrupted by sonication in rosette cooling cell using Branson sonicator 450 (Branson, USA), followed by centrifugation at 15,000 rpm for 10 min at 4°C. The supernatant of cell lysate was loaded onto 5 ml Ni-Sepharose 6 Fast Flow column (GE Healthcare, USA) which had been equilibrated with buffer W. The column was thoroughly washed with the column volume of buffer W containing 50 mM imidazole, and subsequently eluted with buffer W containing 500 mM imidazole. Flow-through, wash, and elution fractions were pooled.

Results

Activity of Fe-S cluster-containing enzymes in mechanically stressed cells

E. coli cells were grown by a fed-batch cultivation system and influences of mechanical stress by PVC particles on bacterial growth and cellular activities of Fe-S cluster-containing enzymes were investigated. Significant decreases both in the growth rate during the log phase and the cell density at the stationary phase were observed in the presence of 100 g/L PVC (Fig. 3-2 (A)) and a leakage of cellular proteins into medium occurred under the stress condition (Fig. 3-2 (B)). These phenomena were consistent with our previous report (Okutani, S., et al 2012).

We measured activities of succinate dehydrogenase and aconitase, both of which have Fe-S cluster essential for their activity, and that of malate dehydrogenase as a control enzyme without the cluster. Activities of the Fe-S cluster-containing enzymes were gradually decreased under the mechanical stress, while levels of the activities in the cells without the stress were kept constant or showed a marginal decrease (Fig. 3-2 (C, D)). No such differential change was seen in the activity of malate dehydrogenase (Fig. 3-2 (E)). These inactivated Fe-S cluster containing enzymes were located in TCA cycle and key players in amino-acids production (Fig. 3-3).

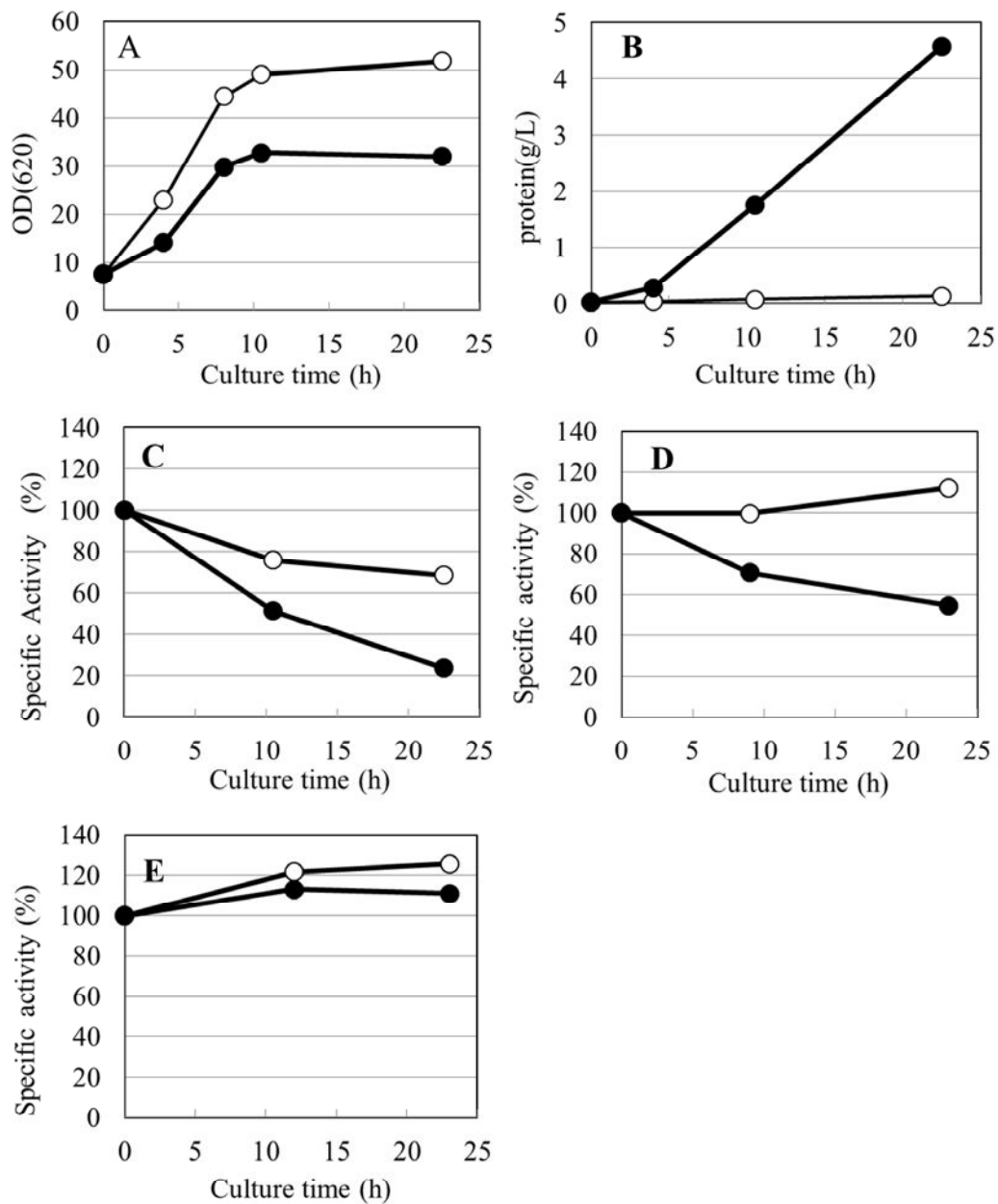


Fig. 3-2 Responses of *E. coli* cells to PVC particle stress throughout all growth phases of fed-batch cultivation.

E. coli cells were cultivated in a fed-batch culture system as described in “Materials and methods” in the presence of 100 g/L PVC particles (closed circles) or absence of PVC particles (open circles). Cell growth was monitored by measuring (A) OD₆₂₀ and (B) extracellular protein concentration at the indicated culture times. Enzyme activities of (C) succinate dehydrogenase, (D) aconitase, and (E) malate dehydrogenase in the extracts from cells grown for the indicated times were measured as described in “Materials and methods” and relative specific activity is presented as the percentage of the activity value of the initial cells. Data are presented as the average of two measurements.

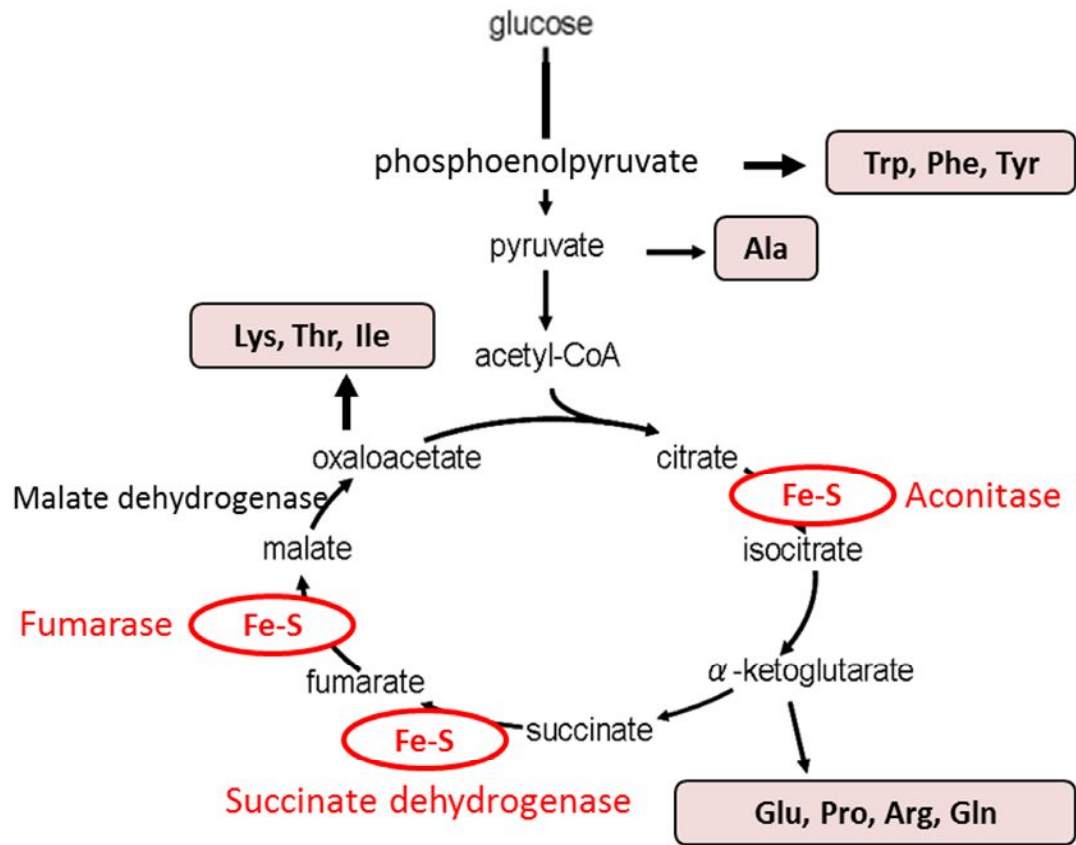


Fig. 3-3 Schematic of metabolic pathway of glycolytic system and TCA cycle

Position in metabolic pathway of Fe-S cluster containing enzymes, succinate dehydrogenase, aconitase, and fumarase, were shown.

It is well documented that damage of cell membrane induces a generation of ROS from bacterial cells (Johnson, D. C., et al 2005). We evaluated the level of ROS, superoxide anion (O_2^-) and hydrogen peroxide (H_2O_2), generation using micro-tube assay. In this micro-tube assay, *E. coli* cells were exposed mechanical stress by vigorous shake in 1.5 ml of micro-tube and protein elution from the cells was observed depending on the amount of PVC particle (Fig. 3-4 (A)). ROS generation from bacterial cells was increased by the mechanical stress of the particle (Fig. 3-4 (B), (C)). As Fe-S cluster is easily decomposed by an attack of ROS (Johnson, D. C., et al 2005), we hypothesized that the predominant decrease in the activities of Fe-S cluster containing enzymes would be a consequence of generation of ROS in the mechanically stressed cells.

To reveal a comprehensive response of bacterial cells to the mechanical stress, we analyzed transcript levels of a total of 4300 genes by using a gene chip (The GeneChip® *E. coli* Genome 2.0 Array, GeneFrontier Corp.). The *E. coli* cells were cultivated with 0 g/L or 100 g/L of PVC particles and harvested after 9 h and 21 h and subjected to preparation of the total RNAs. Genes up-regulated by the stress more than 2 fold were selected from two conditions, early phase and late phase, as described in Fig. 3-5 (A) and 5 genes and 152 genes were selected, respectively. The 5 genes were included within the 152 genes. Gene ontology of the 152 up-regulated genes was shown in Table 3-1 and the up-regulated genes in glycolytic system and TCA cycle were shown in Fig. 3-5 (B).

Many of genes in glycolytic system and a part of genes in TCA cycle were up-regulated by the stress. The bacterial cells might to enhance energy metabolism to survive under the stress condition. The genes encoding aconitase, fumarase and

succinate dehydrogenase were not significantly up-regulated and other genes were up-regulated in TCA cycle. The three genes had Fe-S cluster while genes encoding proteins for Fe-S cluster assembly, including sulfate assimilation and Fe uptake, were increased under the stress condition. These data suggested that cellular ability of the Fe-S cluster assembly might be elevated to retain the activity of Fe-S cluster-containing enzymes. These combined data indicated that almost all enzymes in glycolytic system and TCA cycle were increased gene transcription levels or its cofactor, Fe-S, assembly system.

Table 3-1. Genes up-regulated by mechanical stress of PVC particles

Genes categorized in iron-sulfur cluster assembly are *iscA*, *iscR*, *iscS*, and *iscU*, and other genes in this category, which were up-regulated in a range of 1.4 to 1.8 fold, are *hscA*, *hscB*, *iscX*, and *fdx*.

Gene ontology	Numbers of up-regulated genes
ribosomal protein	45
central metabolism	13
phosphate uptake	12
stress response	12
chaperone	5
RNA polymerase	5
sulfate assimilation	4
iron-sulfur cluster assembly	4
Fe uptake	3
ATP synthase	3
others	24
hypothetical proteins	21

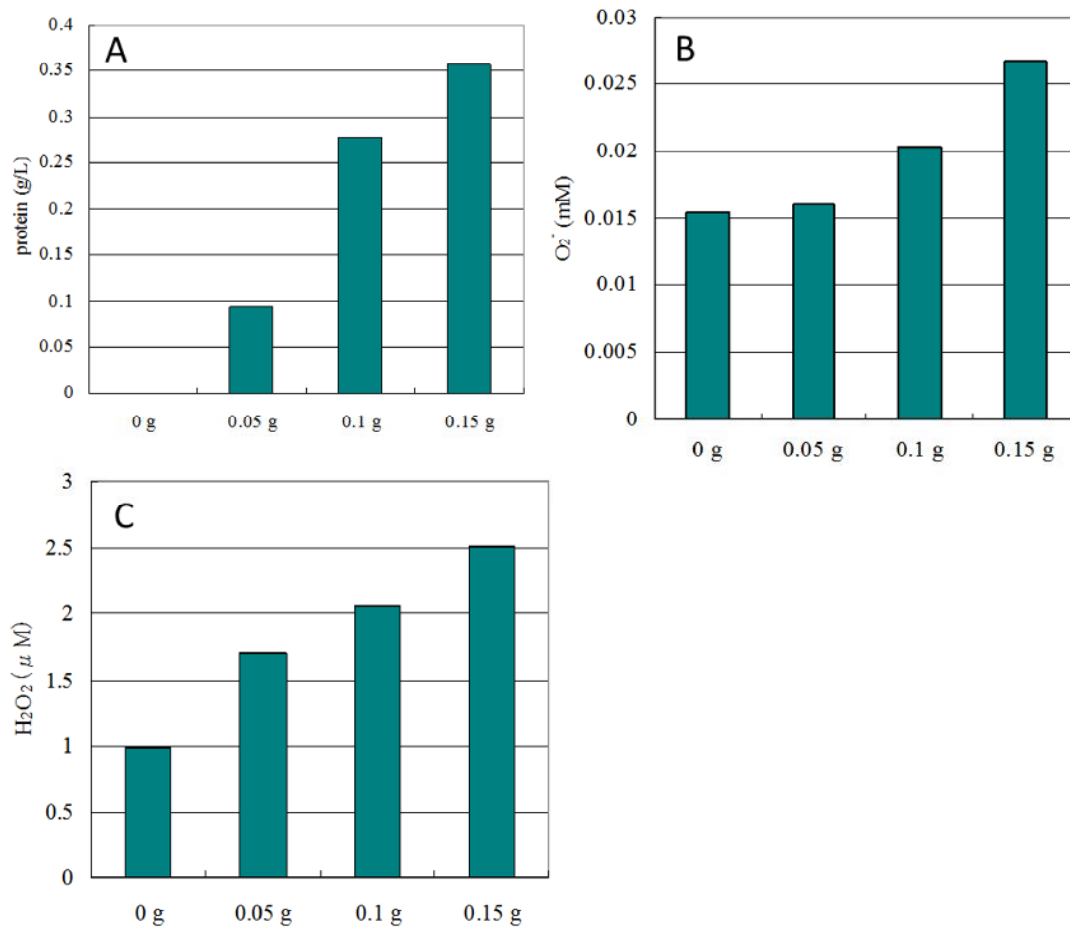
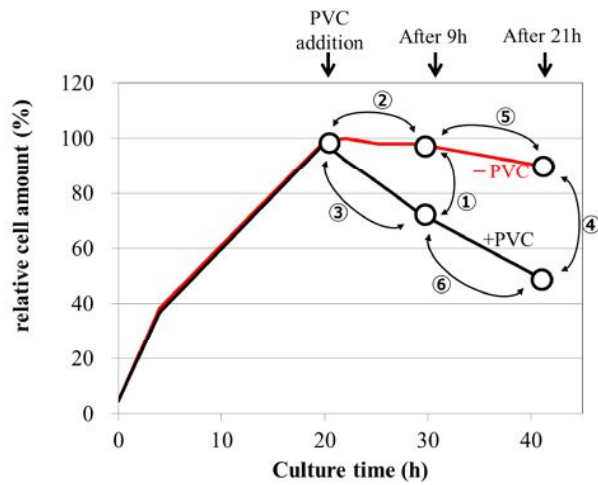


Fig. 3-4 ROS generation under micro-tube assay

(A) Extracellular protein concentration, (B) superoxide anion (O_2^-), and (C) hydrogen peroxide (H_2O_2) were assayed under micro-tube scale mechanical stress assay.

(A)



Selection index of up-regulated genes

Early stage of the stress

- Over two fold on ① and ③ comparison
- No significant change on ② comparison

Late stage of the stress

- Over two fold on ④ and ⑥ comparison
- No significant change on ⑤ comparison

(B)

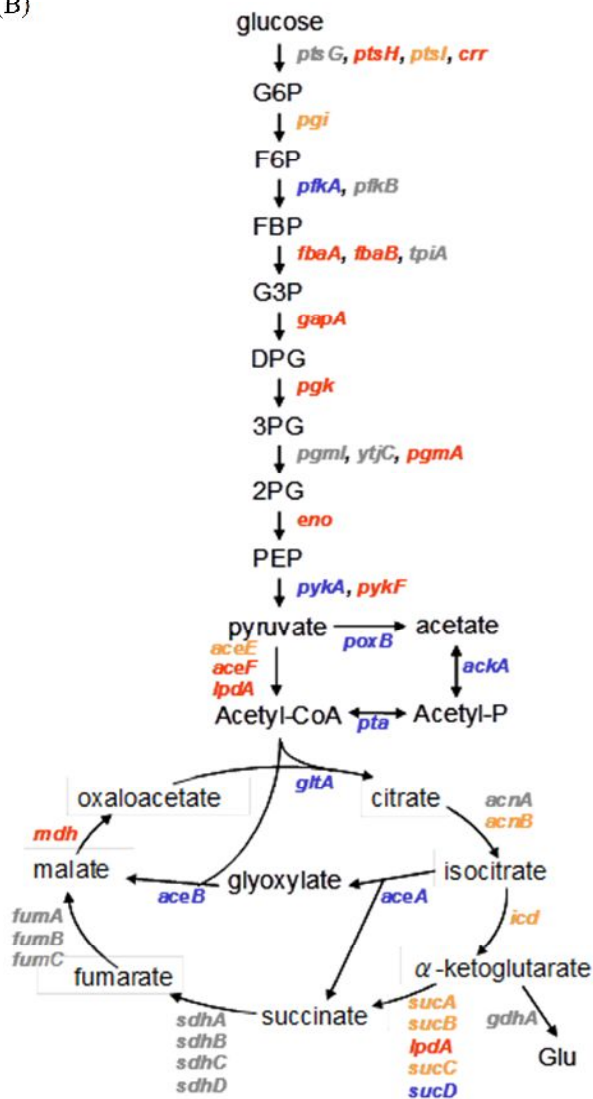


Fig. 3-5 Transcriptome analysis of mechanical stressed cell

(A) Sampling point of cultured cells. The *E. coli* cells cultivated in the presence (+PVC) or absence (-PVC) of PVC particles. The cells were harvested at 9 h and 21 h and subjected to preparation of the total RNAs.

(B) Alteration in gene expression of glycolytic system and TCA cycle. Genes up-regulated over 2-fold were shown in red figure, 1.5~2-fold were shown in orange figure, and 1.0~1.5-fold were shown in blue figure.

Analysis of components of Fe-S cluster assembly machinery

Next, we examined whether expression of components of Fe-S cluster assembly machinery was influenced by the PVC particle stress. The total proteins from *E. coli* cells grown under the stress or non-stress conditions were separated by SDS-PAGE and subjected to immunological detection using specific antibodies against the components of ISC (Fig. 3-6 (A)) or SUF machineries (Fig. 3-6 (B)). Among the components of ISC machinery, HscA showed a remarkable change during cultivation under the stress; new bands smaller than the original band of HscA were appeared in a growth-time dependent manner (Fig. 3-6 (A)) and size differences between the original and the truncated forms were estimated to be 5-10 kDa (Fig. 3-7). No significant change was observed in the expression of HscB, IscA, and IscR of ISC machinery except that a temporal decrease was observed in common at the growth time of 4 h. Regarding components of SUF machinery, SufB seemed to be increased slightly under the stress, but SufA did not show such change.

HscA is a specialized HSP70 chaperon involved in the Fe-S cluster assembly (Vickery, L. E., and Cupp-Vickery, J. R. 2007) and DnaK is also a member of this chaperon which plays a general role in protein folding (Vickery, L. E., et al 1997,

Hesterkamp, T., and Bukau, B. 1998). HscA and DnaK are homologous in the primary and tertiary structures. During cultivation under the PVC particle stress, no detectable change of DnaK was found, showing a marked contrast with HscA (Fig. 3-6 (C)). This suggests that the truncation of HscA is possibly related with its function specialized to the Fe-S cluster assembly.

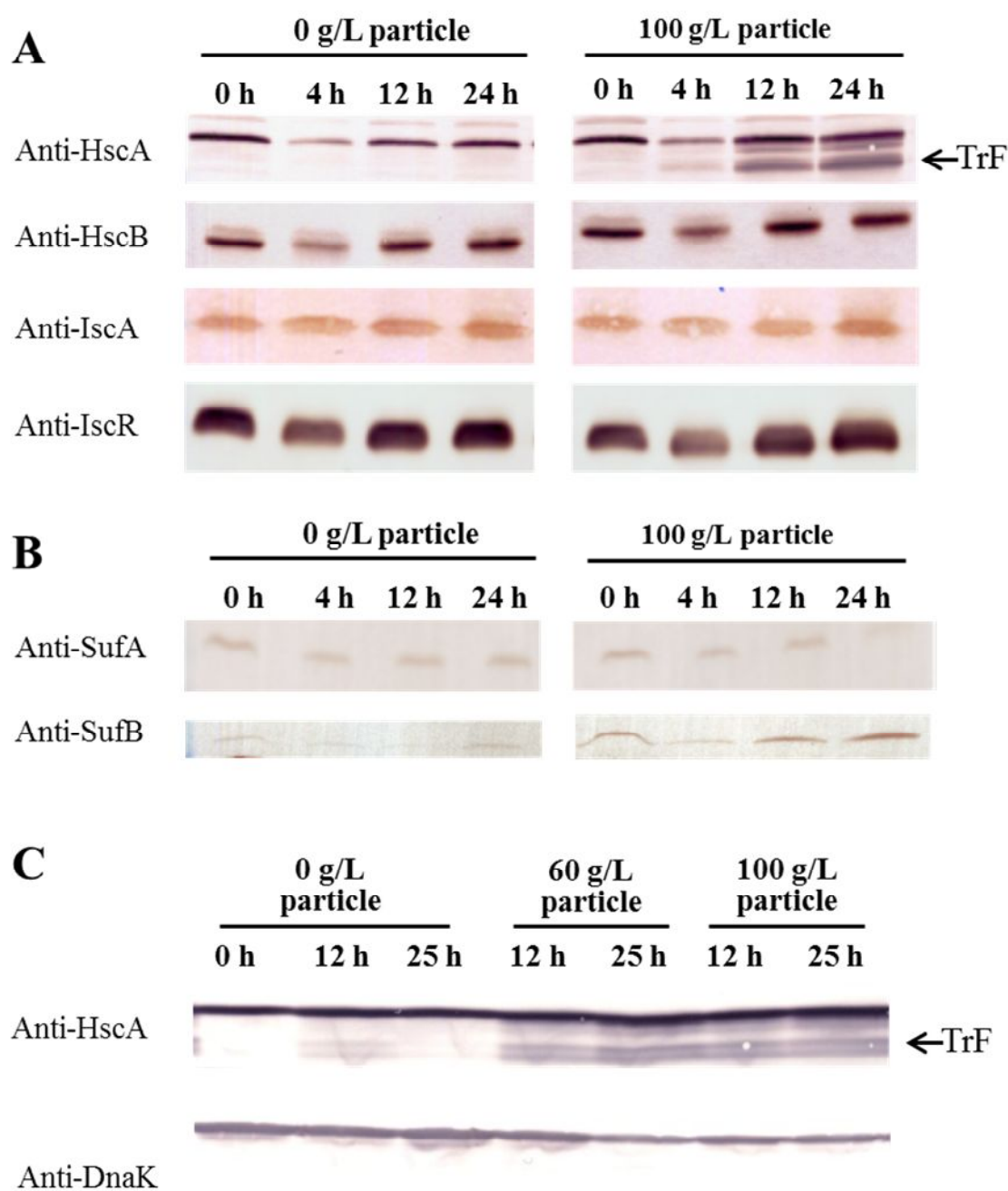


Fig. 3-6 Western blot analysis of the components of Fe-S cluster machineries expressed in *E. coli* cells grown under PVC particle stress.

Total cell extracts were prepared from *E. coli* cells cultivated for 0, 4, 12, and 24 h with 0 g/L or 100 g/L PVC particles as described in Fig. 4-1 and analyzed by western blotting using antibodies against (A) HscA, HscB, IscA, and IscR of ISC machinery and (B) SufA and SufB of SUF machinery. Truncated forms of HscA (TrF) were observed in the cells cultured for 12 and 24 h. (C) To compare HscA with DnaK, a member of HSP70 chaperon, both proteins expressed in the *E. coli* cells cultured under

conditions of PVC particle stress for 12 and 24 h were detected by western blotting using antibodies against HscA and DnaK.

Characterization of the truncation of HscA

We conducted fed-batch cultivation of *E. coli* cells with 30, 60, or 100 g/L of PVC particles to investigate further the truncation of HscA. The result showed that the truncation of HscA was dependent on culture time and dosage of PVC particle stress (Fig. 3-7). No such immunologically detectable polypeptides were seen in *hscA* deleted mutant strain, confirming that the truncated polypeptides were derived from HscA protein (Fig. 3-8).

In order to investigate which terminal end of HscA is trimmed off, *E. coli* cells were transformed with plasmid harboring *hscA* fused with His-tag either at the N-terminus or C-terminus of HscA. Extracts of the two transformed cells were loaded onto Ni-affinity column, washed, and eluted as described in “Materials and Methods”. The flow-through, wash, and elution fractions were analyzed by western-blotting. As shown in Fig. 4-8, both the N- and C-terminal His-tagged HscA of the intact size were bound to the Ni-column, and HscA without His-tag was not bound as being expected. The truncated forms derived from the C-terminal His-tagged HscA was bound to Ni-column (Fig. 3-9). On the other hands, the truncated forms from the N-terminal His-tagged HscA were not bound to the column. These results indicated that the truncation was mainly at the side of N-terminal side of HscA.

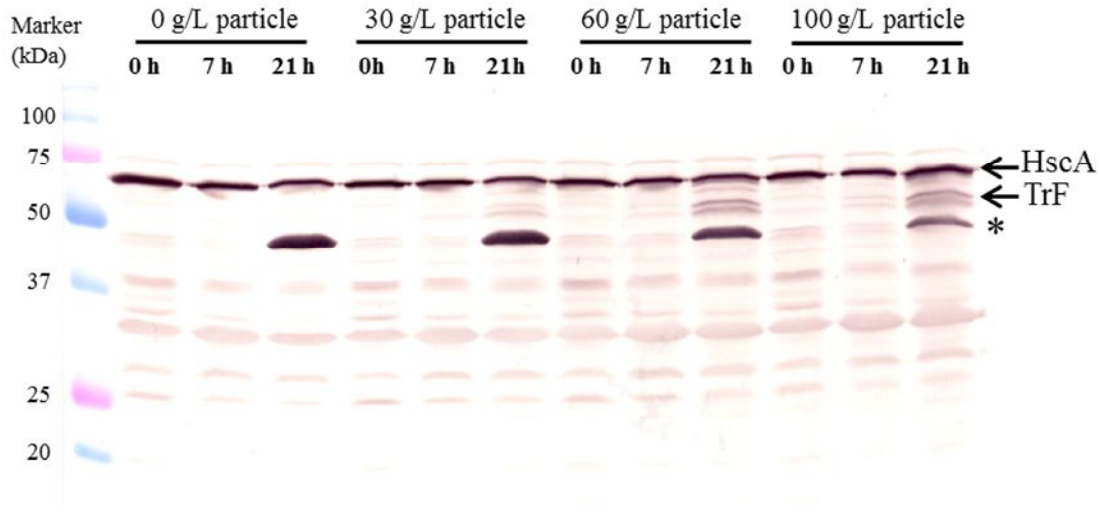


Fig. 3-7 Responses of HscA to variable PVC particle stress.

E. coli cells were pre-cultivated for 2 h and further cultivation was carried out in the presence of increasing amounts of PVC particles (0, 30, 60, and 100 g/L). Cells were harvested at the indicated times of cultivation and expression levels of HscA and its truncated forms (TrF) were analyzed by western blotting using antibodies against HscA. A nonspecific cross-reacted band denoted by star mark (*) appeared in the cells of the late log and stationary phases.

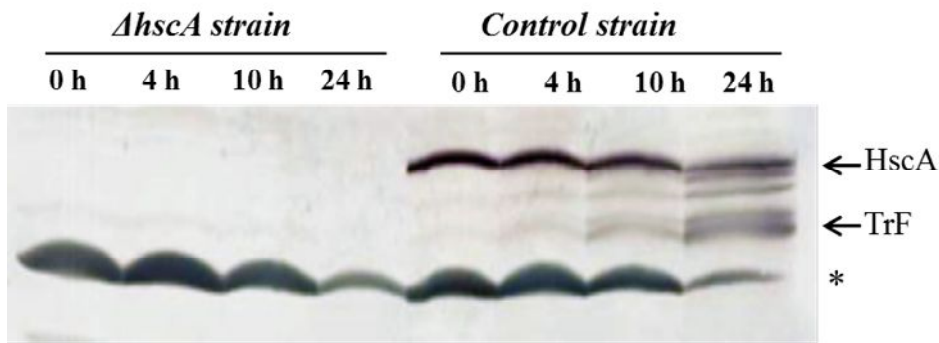


Fig. 3-8 Detection of HscA and its truncated forms (TrF) in *hscA* deficient strain and control strain (*iscX* deficient).

hscA deficient and control strains were pre-cultured for 20 h in the absence of PVC particles. Further cultivation was carried out in the presence of 100 g/L of PVC particles, and cells were harvested at the indicated times, followed by western blotting using antibodies against HscA. Note a nonspecific cross-reacted band denoted by star mark (*) is seen in the cells of all cultivation times, unlike the result shown in Fig. 3-7. This is due to a setting of the pre-culture in this experiment longer than in the experiment of Fig. 3-7, since the growth rate of *hscA* deficient strain was very slow.

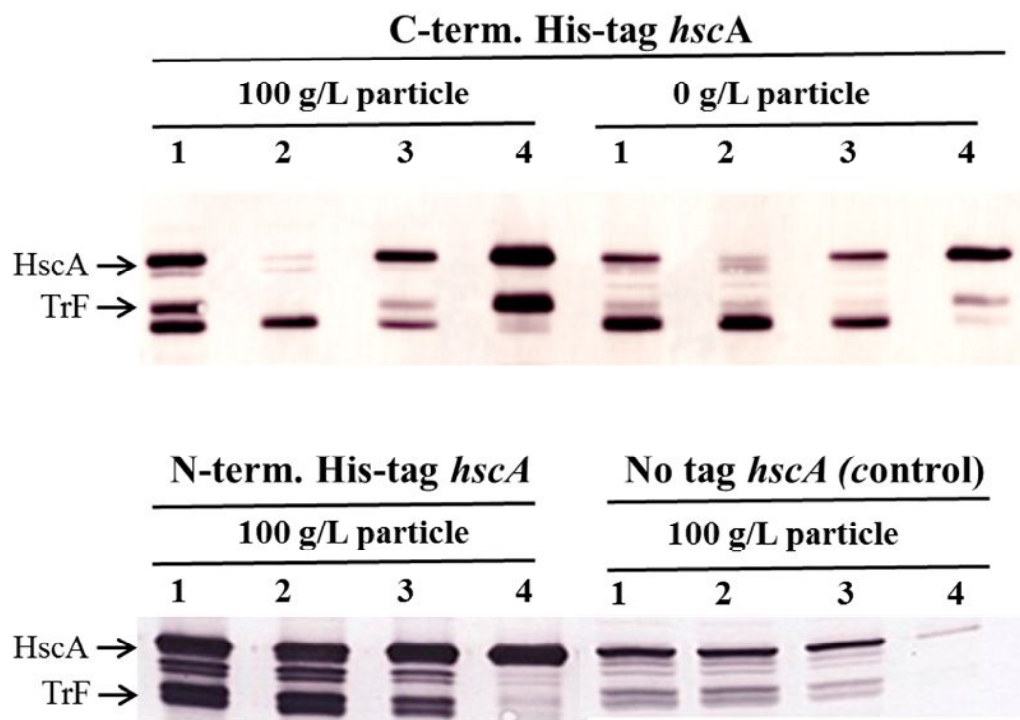


Fig. 3-9 Binding of HscA and its truncated forms to Ni-affinity resin column.

Genes encoding HscA fused with His-tag at its N- or C-termini were introduced into *E. coli* cells. Resulting *E. coli* cells expressing the His-tagged HscAs and the control cells with vector were cultivated with 100 g/L of PVC particles for 24 h. Supernatants obtained from disrupted cells of each strain were loaded onto Ni-column. Supernatant (lane 1), flow through (lane 2), wash (lane 3), and elution (lane 4) fractions were prepared as described in “Materials and methods” and analyzed by western-blotting using antibodies against HscA.

Effect of overexpression of HscA on the mechanically stressed cells

We presumed that HscA should play a role in recovery of damaged Fe-S cluster containing-enzymes in stressed bacterial cells. In order to examine whether this possible function of HscA was enhanced by overexpression of *hscA*, succinate dehydrogenase activity was measured in *E. coli* cells with *hscA* overexpressed. As shown in Fig. 3-10 (A), the *hscA* transformant retained the activity under the stress condition to be higher by approximately 1.7 times than control cells, while no such higher activity was found when grown without the stress. A stress-induced decrease in succinate dehydrogenase activity of the non-transformed cells was not seen, unlike the observation shown in Fig. 3-2(C). This is probably because *E. coli* cells in this experiment were obtained during pre-stationary phase of cultivation. The activity of malate dehydrogenase, a control enzyme was essentially the same irrespective of the *hscA* overexpression. These results showed the overproduction of HscA was effective at least partly for protection of the Fe-S cluster-containing enzyme in the mechanical stressed cells. The overexpression of *hscA* did not give any significant improvement for bacterial growth under the stress condition (Fig. 3-10 (B)).

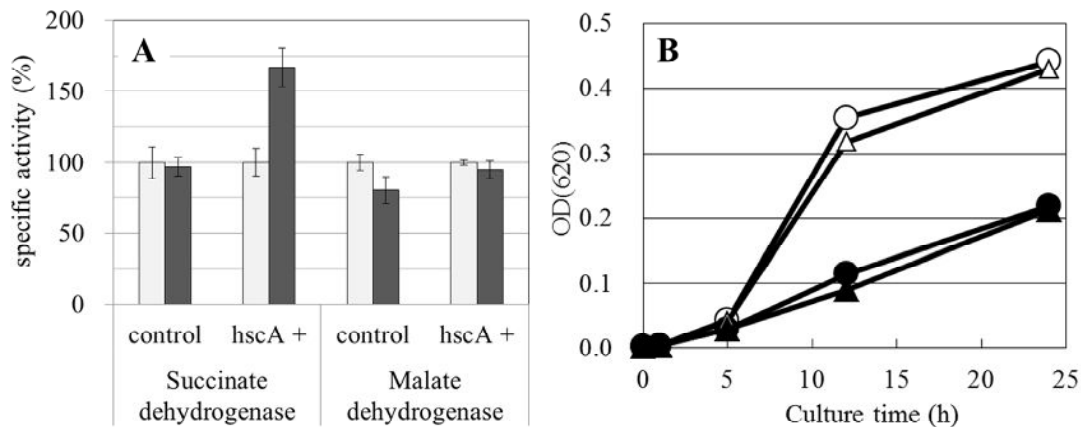


Fig. 3-10 Effect of overproduction of HscA on cellular activity of Fe-S cluster-containing enzyme and cell growth under PVC particle stress during pre-stationary phase of fed-batch cultivation.

(A) *E. coli* strains transformed with plasmid harboring *hscA* gene (*hscA+*) or vector plasmid (control) were cultivated for 24 h with PVC particles of 0 g/L (gray bars) and 100 g/L (black bars). Activities of succinate dehydrogenase and malate dehydrogenase of the 24 h cultured cells were determined and relative specific activity is presented as the percentage of the activity value of the control cells. The error bar represented the standard deviation calculated from triplicate sample. (B) Growth of *hscA* overexpression strain with PVC particles of 0 g/L (open triangles) and 100 g/L (closed triangles), and that of the control strain PVC particles of with 0 g/L (open circles) or 100 g/L (closed circles) were monitored by measuring OD₆₂₀.

Discussion

During amino-acid crystal fermentation, bacterial cells suffer from mechanical stress and productivity yield of amino acids is decreased (Okutani, S., et al 2012). In order to overcome these problems, we have proposed a sophisticated culture system of *E. coli* cells (Araki, M., et al 2008). We also studied physiological responses of *E. coli* cells for being tolerant of the mechanical stress (Okutani, S., et al 2012). This report is a backup for such line of studies by focusing on responses of Fe-S cluster assembly machinery of *E. coli* to the mechanical stress. We observed that activities of succinate dehydrogenase and aconitase, typical enzymes containing Fe-S cluster, were decreased in the bacterial cells suffering mechanical stress. This is most probably due to damage or loss of Fe-S clusters of the enzymes as described in “Results” section.

Regeneration of Fe-S cluster into apo-enzymes requires the cluster assembly machineries of ISC and SUF systems (Wada, K., et al 2010). It is reported that the expression of SUF system, which is kept at a low level under the normal growth condition, is increased in response to oxidative stress, a high temperature shift, and iron starvation (Patzner, S. I., and Hantke, K. 1999, Zheng, M., et al 2001, Outten, F. W., et al 2004). In the present study, the transcriptome analysis of the mechanically stressed cells showed that genes encoding SUF system components did not show any significant change, suggesting the response against the mechanical stress of PVC particles is somewhat different from that against the abovementioned stresses. In contrast, most genes encoding ISC components were up-regulated in the transcription level. However, such general changes were not appreciable at the protein level. Only the protein level of HscA was predominantly altered in response to the PVC particle stress and an interesting phenomenon is an accumulation of the N-terminal truncation forms of HscA

in the stressed cells. The appearance of such truncated forms of HscA has not been reported as far as we know.

A few studies on responses of HscA to several stresses have been reported. The expression of *hscA* was not induced upon heat elevation, but rather induced by temperature shift from 37°C to 10°C or a chloramphenicol addition (Lelivelt, M. J., and Kawula, T. H. 1995). HscA was not essential for viability although the growth of *hscA* defective mutant showed significantly suppressed (Hesterkamp, T., and Bukau, B. 1998). Present study indicates that HscA may play a role in maintenance of Fe-S cluster-containing enzymes under the mechanical stress. Mechanical damage induces membrane injury and metabolic alteration such as temporal increase of glucose-consumption rate and the intracellular ATP concentration (Okutani, S., et al 2012). An enhancement of HscA function would become one of molecular strategies for alleviating metabolic malfunction caused by the mechanical damage. However, growth retardation of bacterial cell under the stress condition could not be rescued only by *hscA* overexpression. Multiple physiological processes of bacterial cells must be negatively influenced by the stress and thus, a combination of Fe-S cluster assembly machinery and other factors would be necessary to give an ability of mechanical tolerance.

Molecular structure of HscA consists of two distinct domains, an N-terminal ATPase activity domain and a C-terminal substrate-binding domain. The ATPase activity of the N-terminal domain is known to be stimulated by interaction with HscB and IscU, and this process greatly influences the rate of cluster transfer (Chandramouli, K., and Johnson, M. K. 2006, Vickery, L. E., and Cupp-Vickery, J. R. 2007). ATPase activity and Fe-S reassembly activity under mechanical stress condition should be affected by N-terminal truncation of HscA by the stress, which might be a specific

response to the mechanical stress. Molecular mechanism how the truncated forms of HscA are involved in the assembly of Fe-S cluster remains open. Further studies of structure and function of HscA and its truncated forms will be necessary.

In conclusion, our current results show that decrease in the level of activities of Fe-S cluster-containing enzymes can be rescued at least partly by the overexpression of HscA. The N-terminal truncated forms of HscA newly appeared during the mechanical stress are closely related with the protection of Fe-S cluster-containing enzymes in the mechanical stressed cells. These findings must be important and useful for our efforts to improve amino-acid crystal fermentation.

Study 3.
Development of a culture process
for efficient amino acid crystal fermentation

Introduction

In our experiment on amino-acid crystal fermentation, the mechanical stress imposed on the bacteria was significantly affected by collision frequency and intensity with the crystals. We evaluated modifications of the culture agitation procedure in an effort to lessen the damage imparted by the crystals and improve fermentation at lower agitation speeds (Fig. 1-5). A reduction in the mechanical stress did not entirely solve the problem because lower agitation speeds often lead to growth retardation because of oxygen deficiency.

Because the intensity of the mechanical stress was determined by the frequency and strength of the crystals colliding with the bacteria, the shape and size of the crystals could be a major factor for the mechanical stress. The mechanical stress exerted by the crystals might be alleviated by adjusting the shape and size of the crystals. In this chapter, we attempted to increase the size of crystals in amino-acid crystal fermentation. We hypothesized that this would reduce the number of crystals, and therefore lessen the collision frequency. Methyl cellulose (MC) was added; this is a chemical agent known to induce a larger size of hydrophobic amino acid crystals in the crystallization process (Inoue, Y., et al 1984).

L-tryptophan is a hydrophobic amino acid that is most commonly used in enhancing animal feed nutrition. Ajinomoto produces approximately 4,500 tons of L-tryptophan per year. The number of L-tryptophan-producing cells of *E. coli* is known to decrease following L- tryptophan crystallization during the fermentation process. In this chapter, we discuss L-Tryptophan fermentation under MC addition. To our knowledge, this is the first study to add MC to the culture medium.

Materials and Methods

Micro-tube assay

The *E. coli* cells were grown on 1.5% agar plates with LB medium containing 1.0% Bacto Tryptone (Becton Dickinson, Franklin Lakes, NJ), 0.5% Bacto yeast extract (Becton Dickinson), and 1.0% sodium chloride, at 37 °C for 24 h. An appropriate amount of the cells were suspended with 50 mM phosphate buffer solution. A 1.0-ml bacterial suspension was transferred to a 1.5-ml micro-tube containing 0.1 g PVC crystals and 2 mg glucose. The micro-tube was placed in a TissueLyser (Qiagen) and shaken vigorously 30 times/s for one hour.

L-tryptophan culture conditions

The L-tryptophan-producing strain of *E. coli*, developed by Ajinomoto, was used. The *E. coli* cells were grown on 1.5% agar plates with LB medium containing 1.0% Bacto Tryptone (Becton Dickinson, Franklin Lakes, NJ), 0.5% Bacto yeast extract (Becton Dickinson), and 1.0% sodium chloride, at 37 °C for 24 h. Approximately 10 µl (one loop) of cells was then transferred into 50 ml LB medium in a 500 ml flask and incubated at 37 °C for 7 h with shaking at 114 rpm on a rotary shaker.

Jar fermenters (Able Corporation, Tokyo, Japan) were used for both seed batch and main fed-batch cultivation. The cultivations were performed under standard laboratory flow conditions. A flask culture (100 µl) was added to a 300-ml batch-cultivation medium. After complete depletion of the initial sugar from the batch cultivation, 30 ml of batch culture was inoculated into 300 ml of fed-batch cultivation medium. These media were designed by Ajinomoto and contained sugar, metals, salts, and hydrolysate. The temperature was maintained at 37 °C, and the pH was maintained

at 7.0 by the addition of gaseous NH₃. Aeration was provided at 300 ml/min throughout the batch and fed-batch cultivation. Following sugar depletion, sugar feeding was started to maintain appropriate glucose concentrations for fed-batch cultivation.

Analytical methods

Cell growth was monitored by measuring OD₆₂₀ using a UV-1600 spectrometer (Shimadzu, Kyoto, Japan) after appropriate dilution with water. The sugar concentration of the culture supernatant was determined using an analyzer BF-5 (Oji Scientific Instruments, Hyogo, Japan). L-tryptophan concentration in culture was analyzed by HPLC with an ODS column. L-tryptophan crystal size was analyzed using the laser particle size analyzer SALD-3000S (Shimadzu).

Chemicals

Various PVC particles (Wako Pure Chemical Industries) were prepared over a size range of three groups using a series of graded sieves. Methyl cellulose 100 (Wako Pure Chemical Industries) was used for this study.

Results

Mechanical stress with various crystal sizes

The effects of crystal size on mechanical stresses were evaluated using several PVC particle sizes. We prepared 3 size ranges of PVC particles: < 54 μm , 77 μm to 110 μm , and 154 μm to 220 μm and examined mechanical stress levels using a micro-tube scale assay system (Fig. 4-1). In this assay, extracellular protein concentrations tended to decrease with particle size (Fig. 4-2) and the protein in the supernatant was detected without any particles. The protein concentration in the 154 to 220- μm particle size condition was decreased by 40% compared with the < 54- μm particle size condition. The mechanical stress levels were reduced by increasing the crystal size. A larger size indicates a smaller number and surface area of crystals with the same weight; therefore, the frequency of collision between the crystals and bacteria would be reduced.

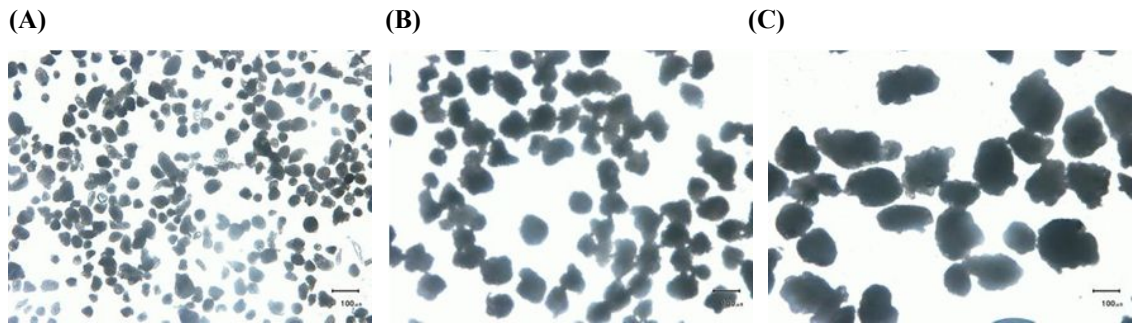


Fig. 4-1 Microscope photograph of PVC particles

(A) $< 54 \mu\text{m}$ (B) $77 \mu\text{m}$ to $110 \mu\text{m}$ (C) $154 \mu\text{m}$ to $220 \mu\text{m}$

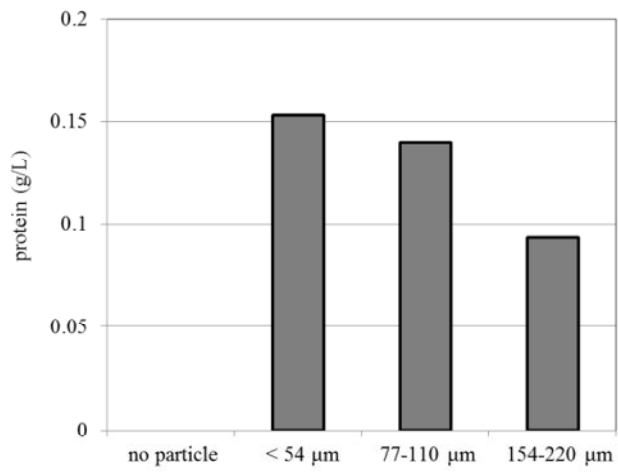


Fig. 4-2 Extracellular protein concentration determined using the micro-tube assay system

Methylcellulose addition to L-tryptophan crystal fermentation

We evaluated the effect of MC addition to the culture medium of L-tryptophan fermentation with respect to an increase in the crystal size and a reduction in the crystal number in order to alleviate mechanical stress caused by the crystals. First, an MC addition of 2.0 g/L into the culture medium was examined. This concentration was set based on the patent (Inoue, Y., et al 1984). However it took a long time to dissolve 2.0 g/L of MC in the medium and heavy foaming occurred during the culture (data not shown). Thus, it seems this concentration is not suitable for the industrial process.

Next, the addition of 70 mg/L and 20 mg/L of MC were examined by L-tryptophan fermentation at 48 h of cultivation. These concentration ranges of MC solution are easy to prepare and foaming was significantly reduced to acceptable levels during cultivation. The average diameters of the L-tryptophan crystals in the broth increased by more than 20% compared with those where MC was not added (Table 4-1).

The number of crystals in the 70-mg/L MC condition was approximately half compared with that where MC was not added. These calculations were based on the assumption that all crystals had a spherical shape, the same average diameter, and similar density. The amounts of *E. coli* cells after crystallization were maintained by the addition of 20 mg/L and 70 mg/L MC (Fig. 4-3).

Table 4-1 Average diameter of L-tryptophan crystals cultivated with 0 mg/L, 20 mg/L or 70 mg/L MC

	MC conc.		
	0 mg/L	20 mg/L	70 mg/L
average crystal size	80 μ m	95 μ m	102 μ m

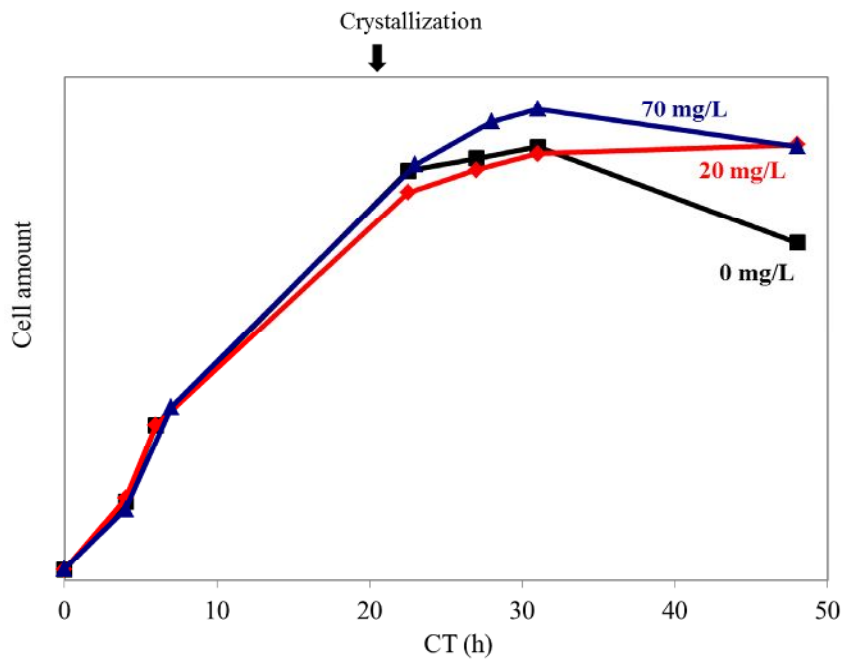


Fig. 4-3 Cell amount profile of L-tryptophan fermentation with the addition of 0 mg/L, 20 mg/L and 70 mg/L MC

Lengthen the culture time to obtain more products

In crystal fermentation, higher amino acid production as crystals is highly beneficial for reducing industry production costs. This is because the amino acid crystals in culture can be used directly as product. However, amino acids dissolved in culture require extraction, purification and the crystallization process.

The total amount of amino acid was not expected to increase significantly because cell amount and production yields decrease after crystallization. Production yield is a value calculated by dividing the amount of product by the amount of consumed sugar. This production yield is directly linked to production costs. Therefore, culture time could not be extended. While cell amounts were maintained after crystallization with the addition of MC, we evaluated the fermentation performance with MC culture under extended cultivation times.

L-tryptophan crystal fermentation was evaluated with the addition of 70 mg/L MC under extended culture time. The results indicated that the enlarged crystal size and increase in cell amount by MC addition were maintained for more than 48 h cultivation (Table 4-2, Fig. 4-4). L-tryptophan yield was maintained with MC for 75 h of cultivation, but there was a 5% decrease in the absence of MC at 75 h compared with 48 h (Table 4-3). Because the yield without MC was reduced at 75 h, it is impossible to extend the cultivation time because of inadequate production. The total amount of L-tryptophan produced with 70 mg/L MC at 75 h cultivation was approximately 40% higher than that without MC at 48 h cultivation.

According to these results, the crystal size of L-tryptophan in the broth was increased by the addition of MC and the mechanical stress exerted on *E.coli* by the crystal was reduced. The bacterial cell number and production yield were maintained

after crystallization and the total amount of L-tryptophan production was improved significantly.

Table 4-2 Average diameter L-tryptophan crystals cultivated with 0 mg/L or 70 mg/L MC at 48 h or 75 h

	0 mg/L MC		70 mg/L MC	
	48 h	75 h	48 h	75 h
average crystal size	80 μm	75 μm	102 μm	100 μm

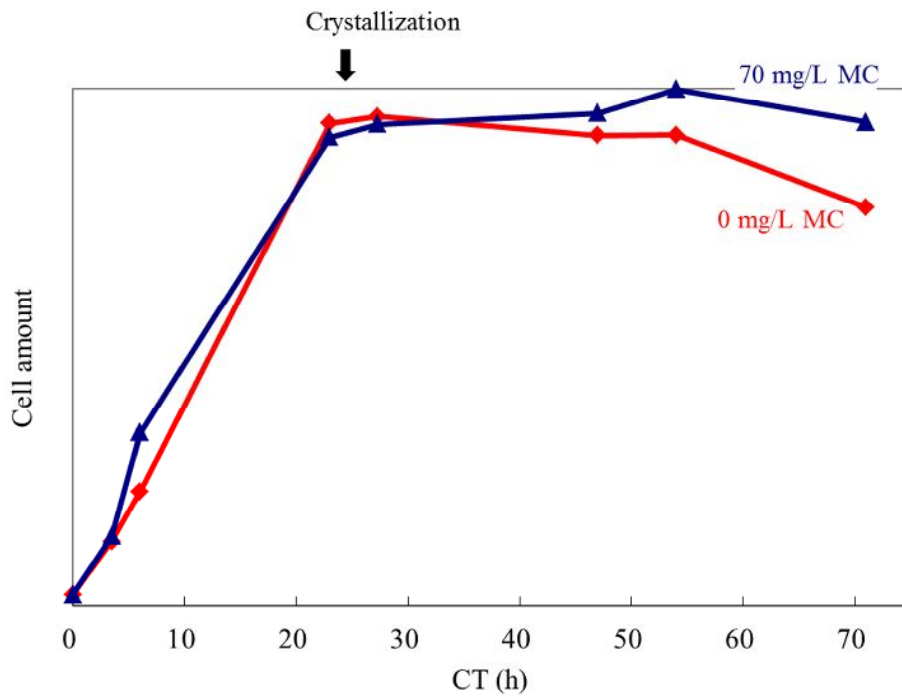


Fig. 4-4 Cell amount profile of L-tryptophan fermentation with 0 mg/L and 70 mg/L MC at 71 h

Table 4-3 Production yield, calculated as the amount of L-tryptophan produced divided by sugar consumed, during fermentation with 0 mg/L or 70 mg/L of MC.

	0 mg/L MC		70 mg/L MC	
	48 h	75 h	48 h	75 h
L-Trp yield	1.00	0.95	1.00	1.02

(The values presented are relative to the yield of 0 mg/L at 48 h, which was designated as 1)

Discussion

MC was used to increase the crystal size of hydrophobic amino acids. This is the first study to control crystal size during amino-acid crystal fermentation. However, we found that high levels of MC caused two problems: 1) heavy foaming was produced during the fermentation process and 2) it was difficult to dissolve the MC in the medium. Subsequently, we optimized the process by reducing the MC concentration in the culture. As a result, these problems were resolved and the L-tryptophan crystal size was increased.

MC prompted an increase in crystal size while simultaneously decreasing the number of crystals; hence mechanical stress was relieved and cell amounts were maintained. When we conducted long-term cultivation with an optimized MC concentration, the production activities of the cells were maintained in the late phase and remarkable improvement of L-tryptophan accumulation was achieved. This process can be also applied to L-phenylalanine fermentation (Okutani, S., et al 2008 patent).

Summary (和文)

細菌は、その生存、増殖の為、様々な温度やpH、栄養源、酸素、浸透圧などの外環境の変化を感知し、それらの変化に適切に対応する機能を有している。本研究ではアミノ酸晶析発酵における細菌への結晶による物理的・機械的なストレスを対象として、生理的・生化学的なストレス応答解析を実施した。アミノ酸晶析発酵とは、発酵培養液中にアミノ酸結晶を析出せしめる培養法のこと、発酵菌は培養液中で結晶とともに攪拌されることで、菌体量低下や生産活性の低下など結晶によるストレスの影響が観察されている。

① モデル培養系の構築とトランスクリプトーム解析

細菌への結晶ストレス応答を解析するため、まずアミノ酸結晶と類似しているポリ塩化ビニル粒子を用いたアミノ酸晶析発酵のモデル培養系を構築した。このモデル培養系を*E. coli*のストレス応答にて評価したところ、アミノ酸晶析発酵と同等の粒子量で、同レベルの菌体量低下が認められ、モデル培養系として成立することを確認した。このモデル培養系にて*E. coli*のストレス応答を解析したところ、糖の取り込み速度の上昇と菌体内ATP濃度の増加が認められた。細菌は結晶によるストレスを感知し、積極的な代謝やエネルギー生産の応答をしていると考えられた。そこで、このストレス応答の全容を解析するため、トランスクリプトーム解析を実施した。その結果、エネルギー生産に重要な解糖系やTCAサイクルを構成する遺伝子群の顕著な転写レベル上昇が認められた。また、結晶ストレス特徴的にFe-S cluster構築に関与する遺伝子の転写レベルの上昇が明らかとなった。Fe-S clusterを保有する酵素は、*E. coli*の生存及びアミノ酸生産にとって非常に重要であることから、Fe-S clusterに着目したストレスの応答解析を実施した。

② Fe-S cluster構築タンパク質のストレス応答

モデル培養系による結晶ストレス応答解析により、活性酸素種(ROS)の発存量増加とFe-S cluster保有酵素の活性低下を見出した。ストレス環境下ではROSによりFe-S clusterが破壊され、Fe-S cluster構築系が上昇しFe-S cluster酵素の活性低下を一定レベルに維持していると示唆された。Fe-S cluster構築に関与する構成タンパク質の発現量をそれぞれ特異的な抗体を用いて免疫学的手法による解析をしたところ、多くはストレスによる顕著な変化は認められなかったが、HscAに5~10 kDa短い新規分子種(HscA*)の発現を新たに発見した。また、N末端もしくはC末端にHis-tagを付与したHscAを用いた解析により、このHscA*はN末端が切断された構造であることを明らかにした。次にHscAの相同性タンパク質で、広くストレス応答に関与することで知られる分子シャペロンDnaKについて結晶ストレス応答を評価したところ、HscAのような有意な応答は認められなかったことから、HscA*の増加は結晶ストレス特異的な現象であり、このストレス環境下でFe-S clusterの再構築に関わっていると考えられた。そこでHscA過剰発現株を構築し、Fe-S cluster保有酵素の活性を測定したところ、ストレス環境下でのみ顕著に酵素活性が上昇することを見出した。通常環境下では有意な変化は認められなかったことから、HscA*がストレス環境下でのFe-S clusterの構築に強く寄与していることが示唆された。

③ 発酵プロセスの改良による結晶によるストレス緩和

結晶ストレスは菌体に対する結晶の接触頻度に大きく影響することから、接触頻度を減らすことでストレスが緩和するのではないかと考え、結晶粒径を大きくし、結晶数を減らす検討を実施した。疎水性アミノ酸の結晶の成長を促す

ことで知られるメチルセルロース(MC)を培養液に添加し、Trp晶析発酵を実施したところ結晶粒径の増大が認められ、培養後半の菌体量や生産活性の維持といった結晶ストレスの緩和が見いだされた。このように、結晶サイズを制御することで、ストレスが軽減できることを証明した。

本研究により、これまで知られていなかったバクテリアのアミノ酸結晶によるストレス応答を分子レベルで生理的・生化学的に解明するとともに、ストレス緩和に向けた応用開発のための基礎的知見を提示することができた。

References

- Abee, T., and Wouters, J. A.:** Microbial stress response in minimal processing, *Int. J. Food Microbiol.*, **50**, 65-91 (1999).
- Addison, A.:** The monosodium glutamate story: The commercial production of MSG and other amino acids, *J. Chem. Educ.*, **81**, 347-355 (2004).
- Agar, J. N., Krebs, C., Frazzon, J., Huynh, B. H., Dean, D. R., Johnson, M. K.:** IscU as a scaffold for iron–sulfur cluster biosynthesis: sequential assembly of [2Fe-2S] and [4Fe-4S] clusters in IscU, *Biochemistry*, **39**, 7856–7862 (2000).
- Ananta, E., Voigt, D., Zenker, M., Heinz, V. Knorr, D.:** Cellular injuries upon exposure of *Escherichia coli* and *Lactobacillus rhamnosus* to high-intensity ultrasound. *J. Appl. Microbiol.*, **99**, 271-278 (2005).
- Ayala-Castro, C., Saini, A., Outten, F. W.:** Fe–S cluster assembly pathways in bacteria, *Microbiol. Mol. Biol. Rev.*, **72**, 110–125 (2008).
- Becker, J., and Wittmann, C.:** Systems and synthetic metabolic engineering for amino acid production - the heartbeat of industrial strain development, *Curr. Opin. Biotechnol.*, **23**, 718-726 (2012).
- Chandramouli, K., and Johnson, M. K.:** HscA and HscB stimulate [2Fe-2S] cluster transfer from IscU to apoferredoxin in an ATP-dependent reaction, *Biochemistry*, **45**, 11087–11095 (2006).
- Chung, H. J., Bang, W., Drake, M. A.:** Stress Response of *Escherichia coli*, *Compr. Rev. Food Sci. Food Saf.*, **5**, 52-64 (2006).
- Cuellar, M. C., Straathof, A. J. J., Van De Sandt, E. J. A., Heijnen, J. J., Van Der Wielen, L. A. M.:** Conceptual evaluation of integrated process configurations for the

recovery of l-phenylalanine product crystals during fermentation, *Ind. Eng. Chem. Res.*, **49** 682-689 (2010).

Deveci, H.: Effect of solids on viability of acidophilic bacteria, *Miner. Eng.*, **15**, 1181–1189 (2002).

Deveci, H.: Effect of particle size and shape of solids on the viability of acidophilic bacteria during mixing in stirred tank reactors. *Hydrometallurgy*, **71**, 385-396 (2004).

Futai, M.: Membrane D-Lactate Dehydrogenase from *Escherichia coli* Purification and Properties, *Biochemistry*, **12**, 2468-2474 (1973).

Gardner, P. R., and Fridovich I.: Inactivation-reeactivation of aconitase in *Escherichia coli*. A sensitive measure of superoxide radical, *J. Biol. Chem.*, **267**, 8757-8763 (1992).

Georgopoulos, C., and Welch, W. J.: Role of the major heat shock proteins as molecular chaperones, *Annu. Rev. Cell Biol.*, **9**, 601–34 (1993).

Glaasker, E., Konings, W. N., Poolman, B.: The application of pH-sensitive fluorescent dyes in lactic acid bacteria reveals distinct extrusion systems for unmodified and conjugated dyes, *Mol. Membr. Biol.*, **13**, 173–181 (1996).

Hackl, R. P., Wright, F. R., Gormerly, L. S.: Bioleaching of refractory gold ores—out of the lab and into the plant. In: Salley, J., McCready, R.G.L., Wichlacz, P.L. *Biohydrometallurgy*. CANMET SP89-10, Canada, 533– 549 (1989).

Hermann, T.: Industrial production of amino acids by coryneform bacteria, *J. Biotechnol.*, **104**, 155–172 (2003).

Hesterkamp, T., and Bukau, B.: Role of the DnaK and HscA homologs of Hsp70 chaperones in protein folding in *E.coli*, *EMBO J.*, **17**, 4818–4828 (1998).

Hoff, K. G., Silberg, J. J., Vickery, L. E.: Interaction of the iron–sulfur cluster assembly protein IscU with the Hsc66/Hsc20 molecular chaperone system of

Escherichia coli, Proc. Natl. Acad. Sci. U.S.A., **97**, 7790–7795 (2000).

Hoff, K. G., Cupp-Vickery, J. R., Vickery, L.E.: Contributions of the LPPVK motif of the iron–sulfur template protein IscU to interactions with the Hsc66-Hsc20 chaperone system, J. Biol. Chem., **278**, 37582–37589 (2003).

Huff, E., Oxley, H., Silverman, C. S.: Density-gradient patterns of *Staphylococcus aureus* cells and cell walls during growth and mechanical disruption, J. Bacteriol., **88**, 1155–1162 (1964).

Iwatani, S., Yamada, Y., Usuda, Y.: Metabolic flux analysis in biotechnology processes, Biotechnol. Lett., **30**, 791-799 (2008).

Johnson, D. C., Dean, D. R., Smith, A. D., Johnson, M. K.: Structure, function, and formation of biological iron–sulfur clusters, Annu. Rev. Biochem., **74**, 247–281. (2005).

Kinoshita, S., Udaka, S., Shimamoto, M.: Studies on amino acid fermentation. part I. Production of L-glutamic acid by various microorganisms, J. Gen. Appl. Microbiol., **3**, 193–205 (1957).

Kobae, Y., Uemura, T., Sato, M. H., Ohnishi, M., Mimura, T., Nakagawa, T. and Maeshima, M.: Zinc transporter of *Arabidopsis thaliana* AtMTP1 is localized to vacuolar membranes and implicated in zinc homeostasis. Plant Cell Physiol., **45**, 1749–1758 (2004).

Kovach, M. E., Elzer, P. H., Hill, D. S., Robertson, G. T., Farris, M. A., Roop, R. M., Peterson, K. M.: Four new derivatives of the broad-host-range cloning vector pBBR1MCS, carrying different antibiotic-resistance cassettes, Gene., **166**, 175-176 (1995).

Kusumoto, I.: Industrial production of L-glutamine, J. Nutr., **131**, 2552S-2555S (2001).

Lelivelt, M. J., and Kawula. T. H., Hsc66, an Hsp70 homolog in *Escherichia coli*, is induced by cold shock but not by heat shock, *J. Bacteriol.*, **177**, 4900-4907 (1995).

Leuchtenberger, W., Huthmacher, K., Drauz, K.: Biotechnological production of amino acids and derivatives: current status and prospects, *Appl. Microbiol. Biotechnol.*, **69**, 1–8 (2005).

Lu, J., Yang, J., Tan, G., Ding, H.: Complementary roles of SufA and IscA in the biogenesis of iron–sulfur clusters in *Escherichia coli*, *Biochem. J.*, **409**, 535–543 (2008).

Mitsubishi, S.: Current topics in the biotechnological production of essential amino acids, functional amino acids, and dipeptides, *Curr. Opin. Biotechnol.*, **26**, 38-44 (2014).

Morris, J. G., Bacterial shock response, *Endeavor* **17**, 2–6 (1993).

Okutani, S., Iwai, T., Iwatani, S., Kondo, K., Osumi, T., Tsujimoto, N., Matsuno, K.: Mechanical damage to *Escherichia coli* cells in a model of amino-acid crystal fermentation, *J. Biosci. Bioeng.*, **113**, 487-490 (2012).

Ollagnier-de-Choudens, S., Sanakis, Y., Fontecave, M.: SufA/IscA: reactivity studies of a class of scaffold proteins involved in [Fe–S] cluster assembly, *J. Biol. Inorg. Chem.*, **9**, 828–838 (2004).

Onda, Y., Matsumura, T., Kimata-Arigo, Y., Sakakibara, H., Sugiyama, T., Hase, T.: Differential interaction of maize root ferredoxin:NADP⁺ oxidoreductase with photosynthetic and non-photosynthetic ferredoxin isoproteins, *Plant Physiol.*, **38**, 225-232 (2000).

Outten, F. W., Djaman, O., Storz, G.: A suf operon requirement for Fe-S cluster assembly during iron starvation in *Escherichia coli*, *Mol. Microbiol.*, **52**, 861-872 (2004).

Patnaik, R., Zolandz, R. R., Green, D. A., Kraynie, D. F.: L-tyrosine production by recombinant *Escherichia coli*: fermentation optimization and recovery, *Biotechnol. Bioeng.*, **99**, 741–752 (2008).

Patzer, S. I., and Hantke, K.: SufS is a NifS-like protein, and SufD is necessary for stability of the [2Fe-2S] FhuF protein in *Escherichia coli*, *J. Bacteriol.*, **181**, 3307-3309 (1999).

Reider, E., Wagner, E. F., Schweiger, M.: Control of phosphoenolpyruvate-dependent phosphotransferase-mediated sugar transport in *Escherichia coli* by energization of the cell membrane, *Proc. Natl. Acad. Sci. USA.*, **76**, 5529–5533 (1979).

Rink, T. J., Tsien, R. Y., Pozzan, T.: Cytoplasmic pH and free Mg²⁺ in lymphocytes, *J. Cell Biol.*, **95**, 189–196 (1982).

Rossi, G.: The design of bioreactors, *Hydrometallurgy*, **59**, 217–231 (2001).

Sano, C.: History of glutamate production, *Am. J. Clin. Nutr.*, **90**, 728S-732S (2009).

Slonczewski, J. L., Rosen, B. P., Alger, J. R., Macnab, R. M.: pH homeostasis in *Escherichia coli*: measurement by ³¹P nuclear magnetic resonance of methylphosphonate and phosphate, *Proc. Natl. Acad. Sci. USA*, **78**, 6271–6275 (1981).

Smith, A. D., Agar, J. N., Johnson, K. A., Frazzon, J., Amster, I. J., Dean, D. R., Johnson, M. K.: Sulfur transfer from IscS to IscU: the first step in iron–sulfur cluster biosynthesis, *J. Am. Chem. Soc.*, **123**, 11103–11104 (2001).

Takahashi, Y., and Tokumoto, U.: A third bacterial system for the assembly of iron-sulfur clusters with homologs in archaea and plastids, *J. Biol. Chem.*, **277**, 28380-28383 (2002).

Thomas, H.: Industrial production of amino acids by coryneform bacteria, *J. biotechnol.*, **104**, 155-172 (2003).

Tokumoto, U., and Takahashi, Y.: Genetic analysis of the *isc* operon in *Escherichia coli* involved in the biogenesis of cellular iron-sulfur proteins, *J. Biochem.*, **130**, 63-71 (2001).

Tokumoto, U., Nomura, S., Minami, Y., Mihara, H., Kato, S., Kurihara, T., Esaki, N., Kanazawa, H., Matsubara, H., Takahashi, Y.: Network of protein-protein interactions among iron-sulfur cluster assembly proteins in *Escherichia coli*, *J. Biochem.*, **131**, 713-719 (2002).

Tokumoto, U., Kitamura, S., Fukuyama, K., Takahashi, Y.: Interchangeability and distinct properties of bacterial Fe-S cluster assembly systems: functional replacement of the *isc* and *suf* operons in *Escherichia coli* with the *nifSU*-like operon from *Helicobacter pylori*, *J. Biochem.*, **136**, 199–209 (2004).

Tsuchido, T., Katsui, N., Takeuchi, A., Takano, M., Shibasaki, I.: Destruction of the outer membrane permeability barrier of *Escherichia coli* by heat treatment, *Appl. Environ. Microb.*, **50**, 298–303 (1985).

Ukeda, H., Shimamura, T., Tsubouchi, M., Harada, Y., Nakai, Y., Sawamura, M.: Spectrophotometric assay of superoxide anion formed in Maillard reaction based on highly water-soluble tetrazolium salt, *Anal. Sci.*, **18**, 1151-1154 (2002).

van Veen, H. W., Abee, T., Kortstee, G. J. J., Pereira, H., Konings, W. N., Zehnder, A. J. B.: Generation of a proton motive force by the excretion of metal-phosphate in the polyphosphate-accumulating *Acinetobacter johnsonii* strain 210A, *J. Biol. Chem.*, **269**, 29509–29514 (1994).

Vickery, L. E., and Cupp-Vickery, J. R.: Molecular chaperones HscA/Ssq1 and HscB/Jac1 and their roles in iron-sulfur protein maturation, *Crit. Rev. Biochem. Mol. Biol.* **42**, 95-111 (2007).

Vickery, L. E., Silberg, J. J., Ta, D. T.: Hsc66 and Hsc20, a new heat shock cognate molecular chaperone system from *Escherichia coli*, *Protein Sci.*, **6**, 1047-1056 (1997).

Volk, C., Albert, T., Kempfski, O.S.: A proton-translocating H⁺-ATPase is involved in C6 glial pH regulation, *Biochim. Biophys. Acta*, **1372**, 28–36 (1998).

Wada, K., Fukuyama, K., Takahashi, Y.: Structure and molecular Mechanisms of Iron-sulfur Cluster Biosynthesis Systems (in Japanese), *Kagaku to seibutsu*, **48**, 831-838 (2010).

Wolfgang, L., Klaus, H., Karlheinz, D.: Biotechnological production of amino acids and derivatives: current status and prospects, *Appl. Microbiol. Biotechnol.*, **69**, 1–8 (2005).

Yura, T., Nagai, H., Mori, H.: Regulation of heat shock response in bacteria, *Annu. Rev. Microbiol.*, **47**, 321–50 (1993).

Zheng, M., Wang, X., Templeton, L. J., Smulski, D. R., LaRossa, R. A., Storz, G.: DNA microarray-mediated transcriptional profiling of the *Escherichia coli* response to hydrogen peroxide, *J. Bacteriol.*, **183**, 4562–4570 (2001).

Zilberstein, D., Agmon, V., Schuldiner, S., and Padan, E.: *Escherichia coli* intracellular pH, membrane potential, and cell growth, *J. Bacteriol.*, **158**, 246–252 (1984).

井上佳美、関守、片桐守、西山博明、小川善司: アミノ酸の晶析法, 特願S59-91826, 公開S60-237054, 公告H5-76463, 1855871, (1984).

List of Publications

Okutani, S., Iwai, T., Iwatani, S., Kondo, K., Osumi, T., Tsujimoto, N., Matsuno, K.: Mechanical damage to *Escherichia coli* cells in a model of amino-acid crystal fermentation, *J. Biosci. Bioeng.*, **113**, 487-490 (2012).

Okutani, S., Iwai, T., Iwatani, S., Matsuno, K., Takahashi, Y., Hase, T.: Response of Fe-S cluster assembly machinery of *Escherichia coli* to mechanical stress in a model of amino-acid crystal fermentation, *J. Biosci. Bioeng.*, (2015). In press

Ishimizu, T., Sasaki, A., Okutani, S., Maeda, M., Yamagishi, M., Hase, S.: Endo- β -mannosidase, a plant enzyme acting on N-glyca: Purification, molecular cloning, and characterization, *J. Biol. Chem.*, **279**, 38555-38562 (2004)

Okutani, S., Hanke, G. T., Satomi, Y., Takao, T., Kurisu, G., Suzuki, A., Hase, T.: Three maize leaf ferredoxin:NADP(H) oxidoreductases vary in sub-chloroplast location, expression, and interaction with ferredoxin, *Plant Physiol.*, **139**, 1451-1459 (2005).

Hanke, G.T., Okutani, S., Satomi, Y., Takao, T., Suzuki, A., Hase, T.: Multiple iso-proteins of FNR in *Arabidopsis*: Evidence for different contributions to chloroplast function and nitrogen assimilation, *Plant Cell Environ.*, **28**, 1146-1157 (2005).

Altmann, B., Twachtman, M. N., Muraki, N., Voss, I., Okutani, S., Kurisu, G., Hase, T., Hanke, G.T.: N-terminal structure of maize ferredoxin:NADP⁺ reductase determines recruitment into different thylakoid membrane complexes, *Plant Cell*, **24**, 2979-2991(2012).

List of Patents

Araki, M., Takahashi, Y., Watanabe, A., Ohnishi, F., Asano, T., Kondo, K., Hibino, W., Iwatani, S., Okutani, S.: 2008. PCT patent WO 2008/102572

Okutani, S., Fujiki, S., Iwatani, S.: 2008. PCT patent WO 2008/04409